Genomic Comparisons of Two *Armillaria* Species with Different Ecological Behaviors and Their Associated Soil Microbial Communities

Jorge Ibarra Caballero
Colorado State University
Bradley M Lalande
Colorado State University
John W Hanna
Rocky Mountain Research Station
Ned B Klopfenstein
Rocky Mountain Research Station
Mee-Sook Kim
Pacific Northwest Research Station
Jane E Stewart (Jane.Stewart@colostate.edu)
Colorado State University https://orcid.org/0000-0001-9496-6540

Research Article

Keywords: Armillaria root disease, tree health, genomes, pathogenic, beneficial fungi, dybiosis

Posted Date: October 18th, 2021

DOI: https://doi.org/10.21203/rs.3.rs-969366/v1

Version of Record: A version of this preprint was published at Microbial Ecology on March 21st, 2022. See the published version at https://doi.org/10.1007/s00248-022-01989-8.

Abstract

Armillaria species show considerable variation in ecological roles and virulence, from mycorrhizae and saprophytes to important root pathogens of trees and horticultural crops. We studied two *Armillaria* species that can be found in coniferous forests of northwestern USA and southwestern Canada. *Armillaria altimontana* is considered as a weak, opportunistic pathogen of coniferous trees, but it also appears to exhibit *in situ* biological control against *A. solidipes*, formerly North American *A. ostoyae*, which is considered a virulent pathogen of coniferous trees. Here, we describe their genome assemblies and present a functional annotation of the predicted genes and proteins for the two *Armillaria* species that exhibit contrasting ecological roles. In addition, the soil microbial communities were examined in association with the two *Armillaria* species within a 45-year-old plantation of western white pine (*Pinus monticola*) in northern Idaho, USA, where *A. altimontana* was associated with improved tree growth and survival, while *A. solidipes* was associated with reduced growth and survival.

Introduction

In recent decades, the genetics of fungal pathogenicity and symbioses have been studied in concert to identify potential patterns related to divergent ecological roles. Genomic comparisons among pathogenic and symbiotic fungi have highlighted great diversity in gene content, genome size, repeat content, and number of chromosomes among fungi with distinct ecological roles [e.g., 1, 2].

Within the Agaricales of basidiomycota, 13,000 species have been described and lifestyles among these range from saprophytes to pathogens to ectomycorrhizal symbionts [3]. Evolutionary studies suggest that ectomycorrhizal lifestyle likely arose from saprophytic fungi [4]. Historically, ectomycorrhizal (ECM) fungi were thought to have reduced numbers of genes encoding plant cell wall-degrading enzymes (PCWDEs), including carbohydrate degrading enzymes. Recent literature has suggested that ECM fungi contain diverse repertoires of these genes encoding PCWDEs [5]. ECM fungi typically retain the distinct suites of PCWDEs and Carbohydrate-Active Enzymes (CAZymes) of their saprotrophic ancestors; some, like the fungal CAZymes acting on pectin (GH28, GH88 and CE8), are expressed in ECM fungi on ectomycorrhizal root tips [5]. Further, little evidence suggests that common gene repertoires exist among ECM fungi [1]. The genome of *Laccaria bicolor*, a well-described ECM fungus, contained twice as many secreted CAZymes [Glycoside-Hydrolases (GH), Polysaccharide Lyases (PL), and Carbohydrate Esterases (C)] than polysaccharide biosynthetic and modifying enzymes [6]; however, this pattern was also observed in the forest root pathogen, *Heterobasidion annosum* [7, 8]. Similarly, both mutualistic and parasitic species of Agaricomycotina typically have an abundance of transposable elements [9]. Thus, differences in genomic content of Agaricales fungi with divergent lifestyles are difficult to detect.

The genus *Armillaria* (Basidiomycota, Agaricales) includes several important plant pathogens of trees/woody plants, but also includes species that are symbionts or even hosts of other organisms [10–12]. *Armillaria* species are also important decomposers in the forests where they occur, especially because they can degrade lignin [11]. Among *Armillaria* species, *A. solidipes* (formerly North American *A.*

ostoyae) is considered one of the more virulent pathogens [13], although virulence varies depending on isolate, host age and other factors [14]. *Armillaria mellea* and *A. borealis* are also considered virulent pathogens, while *A. gallica*, *A. cepistipes*, *A. gemina*, *A. calvescens*, *A. sinapina*, and *A. nabsnona* are considered less virulent or secondary pathogens [10, 12, 15, 16]. A recently described species, *Armillaria altimontana*, formerly North American biological species (NABS) X, is also usually considered as a weak pathogen [17], but evidence for pathogenicity is not well documented [18].

Armillaria solidipes (as *A. ostoyae*) and *A. altimontana* have been documented to co-occur within forest stands in the inland northwestern USA [18–20]. A previous study in northern Idaho, USA provided evidence that *A. altimontana* can provide natural biological control of Armillaria root disease of western white pine (*Pinus monticola*) caused by *A. solidipes*. In this study, *A. solidipes* was uncommon in areas dominated by *A. altimontana*, and trees colonized by *A. solidipes* were associated with a lower growth and survival than trees colonized only by *A. altimontana*. The results demonstrated that *A. altimontana* was not harmful to western white pine within the northern Idaho planting site, and further suggest that *A. altimontana* behaves as a long-term, *in situ* biological control agent against *A. solidipes* [20]. Recognizing the genetic or underlying soil factors that drive host-fungal interactions may provide approaches for enhancing the management of Armillaria root disease.

The distribution, life cycle, pathogenicity, and evolutionary relationships have been studied for several *Armillaria* species [10, 12, 14, 16, 21–25]. Collins et al. [26] studied the genome and proteome of *A. mellea*, identifying carbohydrate degrading enzymes, laccases, and lignin peroxidases among other gene-encoded proteins. Ross-Davis et al. [27] characterized the transcriptome of an *A. solidipes* mycelial fan infecting grand fir (*Abies grandis*), finding high expression of transcripts coding for PCWDEs, along with enzymes and ABC transporters that may help detoxify host-produced defense compounds. More recently, genomes of four *Armillaria* species (*A. cepistipes*, *A. gallica*, *A. ostoyae*, and *A. solidipes*) were sequenced by Sipos et al. [28]; this comparative genomic study revealed a rich repertoire of PCWDEs and pathogenicity-related genes in these *Armillaria* species regardless of their ecological behaviors. This study also identified expression of numerous pathogenicity-related transcripts and proteins during fruiting body and rhizomorph development [24, 28].

Assessing interactions among the soil fungi with different ecological lifestyles (e.g., saprophytes, pathogens, mycorrhizal symbionts, etc.) within the microbial communities is critical to understand disease development. As a well-known example, the association between mycorrhizal fungi and roots that form mycorrhizae allow for increased water and nutrient uptake that sustain tree health [29–33]. Microbes also breakdown litter and forest debris, which maintains forest health by improving soil quality and recycling nutrients that are required by plants [34–38]. In addition, pathogenic soil fungi function as selective agents that can cause mortality to maladapted trees, increasing the vigor and relative adaptation of residual trees in a stand [39–41]. In contrast, highly virulent soil pathogens can infect healthy tree roots, resulting in tree mortality that ultimately degrades the health of forest stands [41]. Additionally, the ability to favor beneficial microbes that inhibit root pathogens, which are notoriously difficult to mitigate, may enhance current management techniques [42, 43].

Soil metagenomics or metabarcoding can be used to identify important fungi, bacteria, and archaea associated with tree health [43]. Determinations of the soil microflora can allow evaluations of treatment (e.g., soil amendments, forest thinning, underburning) influences on naturally occurring microbial communities that favor or suppress forest root diseases/pathogens, which could provide new approaches to manage Armillaria root disease [20, 44, 45].

We present the genome assembly and annotation of the potentially beneficial *A. altimontana* isolated from northern Idaho, northwestern USA, and compare it with the genome of a pathogenic *A. solidipes* isolated from the same region. We also compare the fungal and bacterial communities in the soil associated with two *Armillaria* species – *A. altimontana* and *A. solidipes*. Putative secreted and non-secreted proteins encoded in each of the *Armillaria* genomes and the potential relationship with associated microbial communities are described, with emphasis on genes related to pathogenicity and fungal lifestyles. The data presented here contribute to understanding the ecological function of *Armillaria* species at the genomic level and will serve as resources for understanding genetic and ecological functions of these and other soil fungi.

Materials And Methods

Biological isolates for the genome sequencing. *Armillaria solidipes* [isolate ID001; 27] was obtained from a culture of a basidiospore derived from a fruiting body belonging to a genet that was causing disease via an active mycelial fan growing below the bark of a live grand fir at the Clearwater National Forest, ID, USA. *Armillaria altimontana* (isolate 837-10) was obtained from a basidiospore from a fruiting body collected from the forest soil, with no host tree association ca. 2 km from the same location. Haploid, basidiospore-derived cultures were established for both species.

DNA isolation. Isolates of *A. solidipes* and *A. altimontana* were grown for 3-4 weeks on 0.22 µm-pore MF-Millipore ^{TM} Membrane nylon filters (MilliporeSigma, Burlington, MA) over half-strength "*Armillaria*" culture medium: 1.5% malt extract, 1.5% glucose, 0.5% peptone, 1.2% agar. The fresh mycelia (ca. 1-2 g) was ground by mortar and pestle with liquid nitrogen, and the DNA was extracted with the MoBio (Qiagen) DNeasy PowerMax Soil Kit (Cat.# 12988), following the protocol of the manufacturer.

Genome sequencing and assembly. PacBio sequencing and assembly of the two *Armillaria* species genomes were performed at the Laboratory for Biotechnology and Bioanalysis (LBB), Washington State University. Briefly, 10-15 µg of DNA was sheared using Covaris g-Tubes for 10 minutes at 1,350xg in a Minifuge 16 centrifuge (Beckman Coulter). Approximately, 5 µg of sheared DNA was processed for Pacific Biosciences SMRT bell libraries preparation following the "Procedure and Checklist-20 kb Template Preparation using BluePippin Size Selection System" (P/N 100-286-000-5) protocol (Pacific Biosciences) and the Pacific Biosciences SMRTbell Template Prep kit 1.0 (P/N 100-259-100). Resulting SMRTbell libraries were size selected using a BluePippin gel purification system (Sage Biosciences) according to the Blue Pippin User Manual and Quick Guide. The 0.75% agarose gel cassette was used with a cut-off limit set to 15kb-50kb. The resulting SMRTbell library molecules had an average size of approximately

≥18kb. Appropriate concentrations for the annealing and binding of the SMRTbell libraries were determined using the Pacific Biosciences Binding and Annealing calculator. SMRTbell libraries were annealed and bound to the P6 DNA polymerase for sequencing using the DNA/Polymerase Binding Kit P6 v2.0 (P/N100-372-700), following the recommended protocol from Pacific Biosciences but extending the binding times to 1-3 hours, compared to suggested 30 minutes. The bound SMRTbell libraries were loaded onto the SMRT cells using the standard MagBead protocol, and the MagBead Buffer Kit v2.0 (P/N 100—642-800). Then, the standard MagBead sequencing protocol was followed using the DNA Sequencing Kit 4.0 v2 (P/N 100-612-400) (typically known as P6/C4 chemistry). Sequencing data were collected for 6-hour movie times and Stage Start was enabled to capture the longest single reads possible. Genome assemblies were performed within the Pacific Biosciences SMRT Portal software. HGAPII was used following standard defaults for genome assembly.

Genome assembly and evaluation. Metrics for the genome assemblies, including scaffolds number, total length, GC content, and N50, were obtained using the QUAST [46] web server. Completeness of the assemblies was evaluated using BUSCO 2.0b2 [47]. BUSCO utilizes sets of genes present as single-copy orthologous in a number of species within a clade. For the evaluation of the *Armillaria* genome assemblies, the “Fungi dataset” and the “Basidiomycota dataset” were used. The default e-value of 0.001 was kept for the BLAST searches.

Phylogenetic tree analysis. Whole genome phylogenetic tree was created using Realphy 1.12 [48] with Bowtie2 2.3.3.1 [49] for read mapping and PhyML [50] to build the tree. Preset options were used to run the Realphy pipeline. Whole genome assemblies of *Armillaria* species available at the National Center for Biotechnology Information or the Join Genome Institute websites and the two genome assemblies described in this work were included. The number of bootstrap replicates in PhyML was set to 200.

Structural and functional genome annotations. A set of repetitive sequences was obtained for each of the genome assemblies of *A. solidipes* and *A. altimontana* using RepeatModeler v.1.0.11 [51]. As the first step in the Maker v.2.31.8 pipeline [52], repetitive sequences files were used by RepeatMasker v.4.0.6 [53], to mask and obtain descriptions of interspersed repeats and low complexity DNA sequences. Next, the gene predictors Augustus [54]. GeneMark-ES [55], and SNAP [56] were used for gene prediction in Maker. TRNAscan-SE [57] was also included to predict tRNA genes. For Augustus, a closely related species, *Coprinus cinereus*, was used as species model. SNAP was trained with a set of protein-encoding sequences from *Armillaria* species and closely related species, obtained from the NCBI and EnsemblFungi databases.

The set of proteins generated by Maker was functionally annotated using BLASTp v.2.9.0+ [58] and InterProScan v.5.20-59.0 [59]. Only proteins ≥ 50 amino acids were considered for these and further annotation analyses. For the BLAST search, a database was built with all entries for fungi in the UniProtKB database. A maximum e-value of 0.001 was used. For the InterProScan analysis, the Pfam application was included. Results from BLAST and InterProScan were added to the structural annotation in new gff3 files.

CAZymes were also annotated using the dbCAN2 server [60]; proteins involved in pathogenicity were searched using BLASTp at the PHI database version 46 [61]. Secondary metabolite clusters were annotated using antiSMASH server version 5.1.2 [62] with the detection strictness set to strict, including for the analysis the corresponding genome FASTA file of *A. altimontana* and *A. solidipes*. Deeploc 1.0, a program that utilizes deep learning algorithms [63], was used to predict the set of secreted proteins.

Structural annotation evaluations. Completeness of the *Armillaria* proteomes generated by Maker was evaluated using BUSCO 2.0b2. The “Fungi dataset” and the “Basidiomycota dataset” were used as assessed for the genome assemblies. The default e-value of 0.001 was also kept for the BLAST searches.

Synteny analysis and visualization. Analysis and graphs of synteny blocks (i.e., genomic regions of conserved gene content) were made using SyMAP 2.4 [64, 65]. Genome assemblies and GFF3 files produced by Maker were used to obtain the synteny graphs. Default parameters were used to run the program, except the minimum sequence size was set to 10,000 bp.

Analysis of orthologous protein families. The set of predicted proteins generated by Maker for *A. altimontana* and *A. solidipes* were used to identify orthologous and species-exclusive (non-orthologous) groups using the OrthoVenn2 web server [66]. Two parameters can be adjusted when using the OrthoVenn2 web server: e-value and inflation value; they were set to 1e-10 and 2, respectively. These values were chosen to slightly increase the detection of more non-orthologous proteins compared to the default values (1e-2 and 1.5 respectively).

Study area and field sampling for soil microbial analysis. The study area was located in northern Idaho at the USDA, Forest Service Priest River, Experimental Forest (Supplemental Figure 1). The field site was a historic western white pine seed provenance plot within the Ida Creek study area (ca. 48°21′48.75″ N and 116°49′25.36″ W, elevation ca. 770 m.a.s.l.). In 1971, 2,372 seedlings from Idaho and Washington were planted in a common garden plantation [20]. In 1987, all 2,076 remaining trees were sampled for diameter at breast height (DBH), height, tree health status and association with *A. solidipes* and *A. altimontana*, as described by Warwell et al. [20].

In 2016, 60 trees were randomly selected for sampling, ensuring that half of the trees were historically associated with either *A. solidipes* or *A. altimontana*. Three additional trees (ca. 63) were sampled with needle discoloration and the formation of mycelial fans on the base of the trunk, indicating the presence of *A. solidipes*. Tree measurements included DBH and tree health status, which was based on total amount of needles, color of foliage, insect and disease presence, and dead/live status.

For soil sampling, 1 m from the main stem of a tree near root zones, depths of duff and litter were measured at each cardinal direction in a 30-cm diameter circle. The area was then cleared, and bulk soil samples were taken for each of the 63 trees using a 15-cm, split soil corer with a 15.9-mm (5/8 inch), compact slide hammer (AMS, #400.99, American Falls, ID). Samples were homogenized, 2 g were placed in a 15 ml tube with 5 ml of LifeGuard RNA preservation solution (Qiagen®, Carlsbad, CA), and samples were placed on ice for preservation until storage. Samples were stored at -80C prior to DNA extractions.

Remaining bulk soils from each tree were sent to the USDA Forest Service, Rocky Mountain Research Station, Soils Laboratory in Moscow, ID for soil characteristics measurements and chemistry calculations.

Armillaria rhizomorphs adjacent to the roots were also excavated using a small Pulaski-like gardening tool and brushes. Primary rhizomorph collections occurred on the same side as the soil core while an additional sample was collected 180° on the opposite side of the tree from the core. Rhizomorphs were placed in 15ml tubes and placed on ice or 4°C until isolation and culture.

Armillaria **isolation, DNA extractions and PCR.** Rhizomorphs were plated for fungal isolation within 7 days of collection. Each rhizomorph was surface sterilized by an initial rinse with sterile-distilled water to remove the attached soil particles, followed by a soak in 20% Clorox® bleach solution (1.5% sodium hypochlorite, final concentration) for 6-10 minutes, a rinse with sterile-distilled water and a soak in 3% hydrogen peroxide for 6-10 minutes. After a final rinse with sterile-distilled water, small rhizomorph sections (ca. 1-cm) were plated onto *Armillaria* culture media (3% malt extract, 3% dextrose, 1.5% peptone, 1.5% agar) and incubated at 22°C in the dark to promote mycelial growth.

For DNA extractions from *Armillaria* cultures, mycelia were sub-cultured onto Millipore ™ Membrane nylon filters that overlaid "*Armillaria"* culture medium. After 2-3 weeks, mycelia were scraped off the nylon filters, and DNA was extracted from > 50 mg of mycelia using Zymo Fungal/Bacterial DNA extraction kits (Irvine, CA), following manufacturer protocols with a few modifications. To maximize DNA quantity and quality, three 3-mm glass beads were added to the cell lysis step prior to homogenization (Thermo Savant FastPrep ® FP120 Cell Homogenizer; Qbiogene, Carlsbad, CA) at 6.0 speed with two 30-second cycles. DNA concentration and quality were quantified using a NanoDrop ™ 2000 spectrophotometer (Thermo Fisher Scientific, Wilmington, DE).

For species identification, DNA was amplified at the translation elongation factor-1α (*tef*1) locus using primers EF-983 and EF-2218 [67] with an Eppendorf Mastercycler pro Thermal Cycler (Eppendorf, Hamburg, Germany). The PCR cycle was 94°C for 2.5 minutes, 30 cycles of 94°C for 30 seconds, 60°C for 30 seconds, and 72°C for 1.5 minutes, with a final cycle at 72°C for 10 minutes. PCR products were visualized using gel electrophoresis, cleaned with ExoSAP-IT ™ PCR Product Cleanup Reagent (Thermo Fisher Scientific, Santa Clara, CA), and then Sanger sequenced in two directions by Eurofins Genomics (Louisville, KY). Sequences were edited and aligned in Geneious R11.1 (https://www.geneious.com). Aligned sequences were identified by comparing to the NCBI (National Center for Biotechnology Information) database using BLASTn (https://blast.ncbi.nlm.nih.gov/Blast.cgi) [58].

Soil DNA extraction protocol and sequencing. DNA was extracted from the soil samples preserved in LifeGuard™ Preservation Solution using MoBio Powersoil Total RNA Isolation and DNA Elution Accessory kits (Qiagen®, Carlsbad, CA), following manufacturer protocols. The 15-mL, bead tubes with soil were centrifuged for 5 minutes to separate the soil in the LifeGuard™ Preservation Solution. The LifeGuard™ Preservation Solution was pipetted from the tubes and discarded to leave just the soil. The complete

MoBio Powersoil® manufacturer protocols were followed, resulting in 100 µL of eluted DNA for each sample. DNA qualification and quality were measured using a Nanodrop ^{TM} 2000 spectrophotometer.

Soil DNA (30 µL) was sent to the University of Minnesota Genomics Center and Colorado State University Next-Generation Sequence (NGS) lab for library preparation and sequencing on an Illumina MiSeq and paired-end 2 X 250 reads were generated. A total of 57 out 63 samples were sent for sequencing; the six remaining samples were excluded because they did not yield sufficient DNA concentration/quality. Libraries were prepared for the internal transcribed spacer (ITS2) region to sequence fungal communities and the v4 genomic region of the 16S rRNA to sequence bacterial communities. Primers ITS3 (5'-GCATCGATGAAGAACGAGC-3') and ITS4 (5'TCCTCCGCTTATTGATATGC-3') [68] were used to amplify the ITS2 region, and primers 515F (5'-GTGCCAGCMGCCGCGGTAA-3') and 806R (5'-GGACTACHVHHHTWTCTAAT-3') [69] were used to amplify the v4 region of the 16S rRNA. DNA-free samples were included as negative controls to verify lack of microbial or DNA contamination in the buffers and primer sets. These sequence data have been submitted to the NCBI SRA database under accession number PRJNA767898.

Cleaning DNA sequence data. Data were cleaned to ensure base-calling accuracy of ≥99.9% using the paired end mode in the program Trimmomatic v0.36 [70]. Sequences ≤100bp in length, low quality bases scores (≤15), and 4bp sliding window regions with low average quality scores (≤25) were removed from the data set. The software Mothur v1.40.5 [71] was implemented utilizing the Standard Operating Procedure [72], with some adjustments, to call operational taxonomic units (OTUs) and classification of taxa. Following adjustments described in the SOP (https://github.com/Abdo-Lab/Microbiome-Analysis-Scripts/blob/master/PE-de-novo-processing.pl), UCHIME [73] was used to de novo identify and remove *de novo* chimeric sequences, and USEARCH [74], utilizing the dgc (distance-based greedy clustering) option, was used for clustering. Groups that were at least 97% similar were classified as belonging to the same OTU. Sequences associated with chloroplast, mitochondria, archaea, and bacteria lineages were removed from the table of classified sequences. We utilized the 128 Silva database [75] and the UNITEv6_sh_dynamic_s [76] databases for bacterial and fungal taxonomic classifications, respectively, using Wang's Naïve Bayes classifier with a cutoff value of 80 [77]. Rarefaction curves were generated using the package 'vegan' as implemented in R version 3.6.1 to assess diversity and suitability of depth of coverage per sample [78].

Statistical analysis of communities. Using the RStudio interface to R (R Core Team 2017), alpha diversity, including Shannon diversity index and Inverse Simpson were calculated using phyloseq [79] and rarefied richness (Richness) was determined in Vegan. Shannon's index was used to determine diversity utilizing the relationship to richness and rare microbes [80, 81]. Inverse Simpson was used to identify diversity based on evenness and more dominant microbes to identify diversity [81]. Richness was considered as the number of individuals identified within a single sample, while evenness was used to explain the relative abundance of the different individuals [82].

The relative abundance of taxa associated with *A. solidipes*- and *A. altimontana*-associated soils was determined for the top fungal and bacteria taxa using a stacked bar graph with the metagenomeseq package in R [83]. Differences among communities associated with *Armillaria* species were assessed using a PERMANOVA. Principle component analysis plots were completed in vegan to visualize fungal and bacterial soil differences associated with each *Armillaria* species.

Utilizing relative abundance data based on the resulting OTU table, bar graphs were generated using the ggplot2 package [84] in R for observed taxa with relative abundance > 1% at the genus level to describe the microbial community structure associated with each *Armillaria* species. The MetagenomeSeq package [83] in R was used to fit a model that identified those OTUs associated with significance of model fit at a 0.01 level and minimum fold change of 2 (p values were adjusted for multiple testing). This was used to identify the driver of OTU differences between treatments and time points. Core fungal and bacterial communities were created for each *Armillaria* species. Counts were calculated in R to assess the presence of an OTU corresponding to each species of *Armillaria*. Venn diagrams were produced using molbiotools.com to identify unique and shared fungal and bacterial taxa associated with *A. solidipes* and *A. altimontana*.

To identify influences of what soil chemistry properties on soil fungal communities, a PERMANOVA analysis was completed using the vegan package in R. The analysis identified significant predictors by completing a forward stepwise analysis based on the subset of variables that minimized the Akaike Information Criterion (AIC).

Results

Genome assemblies of A. solidipes **and** A. altimontana. The PacBio assemblies resulted in a 73,739,702 bases genome for *A. altimontana* isolate 837-10 and a 55,735,298 bp genome for *A. solidipes* isolate ID001; both isolates originated near Elk River, Idaho, USA (Table 1). The ratio of genomes sizes, *A. altimontana* / *A. solidipes* = 1.32, is consistent with the ratio of the reported DNA content per nucleus of these two species, 1.34 [19]. The corresponding genome assemblies were deposited at the NCBI with accession number JAIWYR000000000 for *A. altimontana*, and JAIWYQ000000000 for *A. solidipes*.

Table 1
Genome asssembly metrics for *Armillaria altimontana* and *A. solidipes*.

Feature	*A. altimontana*	*A. solidipes*
# scaffolds	100	72
Total length	73,739,702	55,735,298
Largest contig	5,843,527	4,463,803
GC (%)	47.77	48.26
N50	1,930,169	2,424,439

In a whole-genome phylogenetic tree, two *A. solidipes* isolates from North America, ID001and 28-4, group together (Figure 1), apart from but close to isolate C18/9 of *A. ostoyae* from Europe [28]. Figure 1 also shows the position of *A. altimontana* with respect to *A. solidipes* and other *Armillaria* species. *Armillaria altimontana* is contained within a clade comprising *A. cepistipes* B5 and *A. gallica* Ar21-2, which is distinct from the *A. solidipes*/ *ostoyae* clade.

After a custom library of repeats obtained using RepeatModeler was input to RepeatMasker, more bases in *A. altimontana* (18,346,415 bp) were masked compared to those in *A. solidipes* (9,691,790 bp). When comparing *A. altimontana* to *A. solidipes*, the relative proportion of masked bases (1.89) was larger than the ratio of their genome sizes (1.32). The percentage of genomic sequences occupied by interspersed repeats and low complexity DNA regions for *A. altimontana* and *A. solidipes* were 24.88% and 17.39%, respectively (Supplemental Table 1); the largest percentages corresponded to retrotransposons. The most abundant retrotransposons were Long Terminal Repeats (LTRs) as is common in other fungi [85].

Completeness of the genome assemblies was assessed using BUSCO using datasets for both the fungal and basidiomycota lineages. The *A. altimontana* genome assemblywas 95.1% complete when compared to the fungal dataset, and 96.7% when compared to the Basidiomycota dataset. The completeness values for *A. solidipes* were similar at 95.9% and 96%, respectively, and similar to that reported for other *Armillaria* species [28], which indicates high quality for genome assemblies.

Large blocks of shared synteny were found when comparing the *A. altimontana* and *A. solidipes* genomes (Figure 2A shows the 20 largest scaffolds of each species), especially for some of the largest scaffolds of each species (Figures 2B-G). For example, most of *A. altimontana* scaffold 1 (5,843,527 bp) shared synteny with blocks in two *A. solidipes* scaffolds (1 and 2, Figure 2B), most of *A. altimontana* scaffold 2 (5,540,602 bp) shared synteny with blocks in three *A. solidipes* scaffolds (10, 14, and 18, Figure 2C), and most of *A. altimontana* scaffold 3 (4,489,203 bp) shared synteny with blocks in two *A. solidipes* scaffolds (7 and 11, Figure 2D). Likewise, most of *A. solidipes* scaffold 1 (4,463,803 bp) shared synteny with blocks in three *A. altimontana* scaffolds (1, 9, and 13, Figure 2E); most of *A. solidipes* scaffold 2 (4,456,508 bp) shared synteny with blocks in two *A. altimontana* scaffolds (1 and 14, Figure

2F); and most of *A. solidipes* scaffold 3 (4,392,256 bp) shared synteny with blocks in four *A. altimontana* scaffolds (8, 17, 18, and 37, Figure 2G). A number of other smaller complete scaffolds of each species also shared synteny with blocks in one or more scaffolds of the other species (Figure 2A).

Structural and functional annotation. The Maker annotation pipeline predicted several features for the genome assemblies, including CDs, exons, 5'-UTRs, genes, mRNAs, 3'-UTRs, and tRNAs, which were organized in GFF3 files (Table 2; Supplementary Files 1 and 2). High similarity was observed between the genomes of *A. altimontana* and *A. solidipes*. More protein-coding genes were present in the *A. altimontana* genome (19,130 versus 16,105), although the ratio of protein-coding genes, 1.18, is a little smaller than the ratio of genomes sizes (1.32). Despite its smaller genome, the *A. solidipes* genome contained more tRNAs genes (315 versus 280) (Table 2).

Table 2
Genome features of *Armillaria altimontana* and *A. solidipes*

Feature	*A. altimontana*	*A. solidipes*
Genes	19,326	16,357
Average gene length (bp)	1,504	1,563
Gene density (genes per Mb)	262	293
Average exons per gene	5.2	5.6
Average exon length (bp)	219.8	217.2
Average introns per gene	4.2	4.6
Average intron length (bp)	85.9	75.3
tRNA genes	280	315
transcripts/proteins*	19,130	16,105
* some genes are predicted to code for more than one protein		

Completeness of the predicted proteomes was assessed using BUSCO, again with datasets for both the fungal and Basidiomycota lineages. For *A. altimontana*, proteome completeness was 96.9% when compared to the fungal dataset, and 96.4% when compared to the Basidiomycota dataset. Proteome completeness values for *A. solidipes* were 97.2% and 96.7%, respectively, indicating high quality of the genome structural annotations.

Predicted proteins sets for *A. altimontana* and *A. solidipes* (Supplementary Files 3 and 4) were functionally annotated using BLASTp against all the fungi entries in the Uniprot database, and by using InterProScan including the Pfam application. These results were added to the final genome models produced by Maker, in GFF3 format (Supplementary Files 1 and 2). For *A. altimontana*, 17,997 encoded proteins had a BLASTp hit, and 8,483 had an InterProScan (Pfam) hit (94.0% and 44.3% of the total,

respectively). For *A. solidipes*, 15,449 encoded proteins had a BLASTp hit, and 8,132 had an InterProScan (Pfam) hit (95.9% and 50.4% of the total, respectively).

In comparisons with other *Armillaria* proteomes, 9,061 *A. altimontana* isolate-encoded proteins had a BLASTp hit to *A. gallica* proteins, 4,723 to *A. ostoyae* proteins, and 3,906 to *A. solidipes* proteins (8,629 to *A. ostoyae*/*solidipes* proteins) (Supplementary Files 3 and 4). For our *A. solidipes* isolate-encoded proteins, only 1,321 had a BLASTp hit to *A. gallica* proteins, 6,665 to *A. ostoyae* proteins, and 7,300 to other *A. solidipes* proteins (13,795 to *A. ostoyae*/*solidipes* proteins).

Secreted proteins. The program Deeploc was used to obtain corresponding sets of putative secreted proteins of *A. altimontana* and *A. solidipes* to search for differences that might reflect the lifestyle differences. A total of 1,235 (6.4% of the total) secreted proteins were predicted in *A. altimontana* and 1,157 (7.1%) were predicted in *A. solidipes*. In *A. altimontana*, 322 secreted proteins had a CAZyme annotation; and 2 were cytochrome P450; in *A. solidipes*, the number of hits in each category were similar: 316 as CAZYmes; and 3 were cytochrome P450. No secreted proteins from either species had a blast hit with identity above 95% to proteins in the PHI database (data not shown). Some of the proteins had a CAZyme and a BLASTp hit, with one or several hits in the InterProScan search. But 99 secreted proteins in *A. altimontana* produced no hits and other 436 produced only BLASTp hits to uncharacterized proteins; in *A. solidipes*, 69 secreted proteins produced no hits and other 421 produced only BLASTp hits to uncharacterized proteins. However, many of these uncharacterized proteins could be considered “small secreted proteins” (see below). All those different annotations were combined and manually curated (Supplemental Files 3 and 4).

Numbers of secreted proteins with putative involvement in pathogenicity were obtained for each *Armillaria* species. The differences between the two species were small (Supplemental Figure 2); the two major differences were a higher number of peptidases secreted by *A. solidipes* and a higher number of small secreted proteins for *A. altimontana*.

When grouped by probable function (Figure 3), the major differences in predicted secreted proteins of *A. altimontana* and *A. solidipes* were associated with cell wall-degrading enzymes. *Armillaria solidipes* showed a slightly larger number of enzymes that degrade plant cell wall components: cellulose, hemicellulose, lignin, and especially pectin. Encoded-protein degrading enzymes also were more abundant in *A. solidipes* compared to *A. altimontana* (Figure 3). Abundances of other encoded protein categories showed smaller differences.

The number of encoded proteins that could be considered “small secreted proteins”, defined as those smaller than 300 amino acids (after being predicted as “extracellular”), were 678 (~55% of total secreted) in *A. altimontana*, 381 with at least 2% cysteine residues; and 594 (~51% of total secreted) in *A. solidipes*, 334 with at least 2% cysteine residues. Numerous encoded small secreted proteins (205 in *A. altimontana* and 172 in *A. solidipes*) were annotated as CAZymes, peptidases, thaumatin, cerato-platanin, hydrophobins, etc. (Supplemental Files 3 and 4); however, for other predicted small secreted proteins (375 in *A. altimontana* and 353 in *A. solidipes*) the only annotation were BLASTp hits to “Uncharacterized

protein", and there was no annotation for other predicted proteins (98 in *A. altimontana* and 69 in *A. solidipes*).

Non-secreted proteins. Numerous different functions were found among encoded proteins considered as non-secreted. Among them, those that matched CAZymes, cytochrome P450, transporters or secondary metabolite clusters were further examined (Table 3). Transporters and secondary metabolites clusters were also included in these analyses because they have also been considered important for the lifestyle of fungal species [86, 87]. The abundance of encoded proteins annotated as CAZymes, ABC transporters and secondary metabolite clusters were similar between *A. altimontana* and *A. solidipes* (Table 3); whereas numbers of cytochrome P450 and all transporters were larger in *A. altimontana*. However, the ratio *A. altimontana* / *A. solidipes* encoded protein numbers for most categories was smaller than the ratio of the genome sizes (1.32) and total proteins (1.18); only cytochrome P450 ratio was slightly higher (1.25) than the ratio of total proteins (Table 3).

Table 3
Total number of non-secreted proteins by gene family for *Armillaria altimontana* and *A. solidipes*. The genome sizes were included for comparison.

Feature	*A. altimontana*	*A. solidipes*	ratio
Total non-secreted	17,895	14,948	1.19
CAZymes-cytochrome P450	334 - 242	305 - 195	1.09 - 1.25
Total transporters	474	414	1.14
ABC transporters	67	60	1.11
Secondary metabolite clusters	21	19	1.10
Total proteins	19,130	16,105	1.18
Genome size	73,739,702	55,735,298	1.32

When the abundance of the non-secreted CAZymes was grouped by substrate, the largest differences were found within encoded pectin-degrading enzymes with 58 in *A. altimontana* and 47 in *A. solidipes*; carbohydrate binding with 17 and 8 respectively; and lignin degrading enzymes with 49 and 41 respectively (Supplemental Figure 3). Overall, most non-secreted CAZymes numbers were typically higher in *A. altimontana* in comparison with *A. solidipes*.

Genes upregulated in rhizomorphs. We searched for genes reported by Sipos et al. [28] as notable genes that were upregulated in rhizomorphs. Most of the categories had similar numbers between both *Armillaria* species, although *A. altimontana* possessed 62 more genes encoding cytochrome P450 (Table 4). A diversity of functions has been ascribed to Cytochrome P450 proteins [88–91]. Caspase domain-containing proteins, part of proteases that have been associated with programed cell death in other

organisms [92], were more abundant (10 more) in *A. solidipes*. Relatively large differences were also found in numbers of genes encoding two enzymes involved in secondary metabolites synthesis: polyprenyl synthase, involved in terpenoid synthesis [93, 94], had 23 in *A. altimontana* versus 12 in *A. solidipes*; while trichodiene synthase, which utilizes terpenoids to produce the trichodiene [94] was more abundant in *A. solidipes* with 12, versus only 3 in *A. altimontana* (Table 4).

Table 4
Number of notable genes with overexpression in rhizomorphs (Sipos et al. 2017; 27) in the Armillaria altimontana and A. solidipes genome assemblies.

protein coded (Pfam terms)	*A. altimontana*	*A. solidipes*
expansin (PF03330)	12	8
bzip transcription factor (PF00170)	5	5
zinc finger c2h2 (PF00096, PF12874, PF12756, PF06220, PF16278, PF08790)	62	68
caspase domain (PF00656, PF14538)	30	40
hydrophobin (PF01185)	7	4
cytochrome P450 (PF00067)	271	209
GH28 (PF00295)	17	16
pectinesterase (PF01095)	9	10
GH88 (GH105) (PF07470)	6	5
PL3 (PF03211)	9	10
GH3 (PF00933)	16	14
GH43 (PF04616)	11	10
GH76 (PF03663)	6	5
AA9 (PF03443)	18	21
Total cellulases	183	179
cellulase (PF00150)	19	19
POD (PF00141; PF11895)	10	11
HTP (PF01328)	6	6
laccase (PF00394)	25	28
cerato-platanin (PF07249)	4	4
carboxylesterase (PF00135)	32	37
family 6 bacterial extracellular solute-binding protein (PF13343)	2	1
polyketide synthase (PF14765)	10	7
trichodiene synthase (PF06330)	3	12
polyprenyl synthase (PF00348)	23	12

Orthologous and non-orthologous proteins. Although approximately 62% of *A. altimontana* and 72% of *A. solidipes* proteins grouped in 10,989 clusters of orthologous proteins, a large number, 7,232, of proteins were non-orthologous in *A. altimontana*, and 4,575 were non-orthologous in *A. solidipes* (Figure 4).

Out of the 10,989 clusters of orthologous proteins, 10,321 were two protein clusters, made from one protein from each species; only 29 clusters had a difference larger than 5 proteins. Of those, 24 cluster had more *A. altimontana* proteins, whereas there were five clusters that *A. solidipes* had a greater number of proteins. Out of those 29 clusters, one of them contained CBM67 proteins, which bind rhamnose residues in pectin, with 15 proteins from *A. altimontana* versus only one from *A. solidipes*. Another cluster contained ABC transporters, of which, *A. altimontana* also had ten more than *A. solidipes*. Two clusters contained caspase-domain proteins, with 17 more from *A. solidipes* than from *A. altimontana*. Other clusters corresponded to transposases, transcription factors, helicases, F-box proteins, and histone-modifying enzymes, while no annotation was found for 14 clusters (Table 5).

Table 5
Orthologus and non-orthologous proteins in Armillaria altimontana – Armillaria solidipes comparison. Only information for proteins with count difference larger than 5 were included, except for non-orthologous terpene synthase and transcriptional activator of glycolytic enzymes with 4 present only in A. altimontana.

Orthologous proteins				
2 protein clusters	10,321			
3-5 protein clusters	576			
> 5 protein cluster	29			
cluster_name	protein number	annotation	*A. altimontana*	*A. solidipes*
cluster1	30	transposase	28	2
cluster6	19	BTB/POZ domain protein, maybe transcription factor	18	1
cluster12	16	CBM67, rhamnose binding in polysaccharides (pectin)	15	1
cluster13	16	only one protein with: Zinc kucle domain	15	1
cluster2	21	helicase, involved in telomere maintenance	15	6
cluster4	21	no annotation	14	7
cluster19	14	no annotation	13	1
cluster14	15	no annotation	13	2
cluster27	13	F-box domain protein, different functions including fungal pathogenesis	12	1
cluster31	12	no annotation	11	1
cluster30	12	ABC transporter	11	1
cluster24	13	no annotation	11	2
cluster53	10	no annotation	9	1
cluster55	10	only one protein with: uncharacterized domain	9	1
cluster61	9	no annotation	8	1
cluster63	9	transposase	8	1
cluster68	9	no annotation	8	1

Orthologous proteins				
cluster70	9	no annotation	8	1
cluster73	9	no annotation	8	1
cluster74	9	no annotation	8	1
cluster79	9	helicase, involved in telomere maintenance	8	1
cluster54	10	no annotation	8	2
cluster44	10	SET domain protein, histone modifying enzymes	8	2
cluster81	8	no annotation	7	1
cluster40	11	only three proteins with: domain of unknown function	2	9
cluster10	19	F-box domain protein, different functions including fungal pathogenesis	2	17
cluster99	8	caspase domain protein	1	7
cluster100	8	no annotation	1	7
cluster28	13	caspase domain protein	1	12
Non-orthologous proteins				
	A. altimontana	*A. solidipes*		
Cazymes	91	80		
Cytochrome P450	87	48		
Other proteins with count difference > 5				
polyprenyl synthase	15	6		
trichodiene synthase	2	11		
F-box protein	81	52		
glutathione S-transferase	1	11		
Clp amino terminal domain, pathogenicity island component	6	0		

Orthologous proteins		
DDE superfamily endonuclease	8	0
Sodium/hydrogen exchanger family	0	8
Secreted proteins/small secreted proteins	344/327	265/248
Exclusive with possible host-interaction function		
terpene synthase	4	0
transcriptional activator of glycolytic enzymes	4	0

CAZymes and cytochrome P450 enzymes were found among non-orthologous proteins. The number of non-orthologous CAZymes was 91 in *A. altimontana* and 80 in *A. solidipes*, with small differences in number of individual CAZymes between the two species, which is similar to the differences found in secreted and in non-secreted CAZymes. A few non-orthologous CAZymes were exclusive, but only GT32 was found exclusively in *A. altimontana* among CAZymes with a count of greater than 5. For cytochrome P450, the difference was larger: 39 more in *A. altimontana* (Table 5); slightly smaller than the difference, 46, of total cytochrome P450 proteins (244 in *A. altimontana* vs 198 in *A. solidipes*).

Many other proteins that were present in both *A. altimontana* and *A. solidipes* with the same Pfam-Interpro annotation were still considered non-orthologous by OrthoVenn2, and their numbers were also similar in most cases. Those with a number difference greater than 5 included polyprenyl synthase, trichodiene synthase, F-box protein, and glutathione S-transferase. Other proteins were present only in one *Armillaria* species, most of them occurred in small numbers: three with counts greater than 5: Clp amino terminal domain pathogenicity island component, and DDE superfamily endonuclease, only in *A. altimontana*; Sodium/hydrogen exchanger family, only in *A. solidipes*. Other non-orthologous proteins with smaller numbers, but with a possible host-pathogen interaction function, included terpene synthase (4) and transcriptional activator of glycolytic enzymes (4), which were found only in *A. altimontana*.

Finally, 344 *A. altimontana* non-orthologous proteins were predicted as secreted with 327 of them as small secreted proteins. For non-orthologous proteins from *A. solidipes*, 265 were predicted as secreted with 248 of them as small secreted protein (Table 5).

Armillaria **species identified from field plots.** Rhizomorphs were isolated from 51 total trees, yielding 87 rhizomorph samples that all produced pure *Armillaria* cultures. Sequencing the *tef1* gene from the 87 rhizomorph samples resulted in 48 trees associated with *A. altimontana*, 3 trees associated with *A. solidipes*. Twelve trees resulted in unsuccessful rhizomorph isolation, therefore these samples were not

utilized in analyses. Sequences corresponding to both *A. altimontana* and *A. solidipes* resulted in 99% identity during blast searches on the NCBI database.

Processing sequenced 16S and ITS2 libraries in Mothur. From the soil samples, a total of 2,156,476 and 4,323,028 raw paired-end 2 x 250bp reads from 56 samples were generated from 16S and ITS sequencing, respectively. For the 16S dataset, the mean sequencing depth after processing was 27,639 reads/sample, with a range from 6 to 107,582. Eighteen samples yielded < 5,000 total reads and were removed from analyses for the 16S dataset. For the ITS dataset, the mean sequencing depth after processing was 51,806 reads/sample, with a range from 15,017 to 77,969. The total datasets yielded 26,781 and 6,936 OTUs for the 16S and ITS2, respectively. The resulting rarefaction curves for these 16S sequence data indicating adequate sampling depth (Supplementary Figure 4). Matching to the Silva database resulted in a16S dataset of 6,677 unique OTUs and matching to the UNITE database resulted in an ITS2 dataset of 2,806 unique OTUs.

Analyses of microbial communities. Samples were grouped into treatments associated with species of *Armillaria* (*A. altimontana* or *A. solidipes*). Non-metric, multidimensional scaling (NMDS) plots indicated that soil bacterial communities differed more than the fungal communities associated with both *A. altimontana* and *A. solidipes* (Supplemental Figure 4).

Differences in community alpha diversity and richness. Bacterial and fungal communities were assessed for overall rarefied richness and diversity. We did not observe significant differences in richness among soil fungal communities associated with *A. solidipes* or *A. altimontana* ($F_{(1,52)}$ = 0.0462, P = 0.8310). Additionally, we did not observe significant fungal differences for either diversity index (Shannon's or Inverse Simpson) associated with *A. solidipes* or *A. altimontana* ($F_{(1,52)}$ = 0.16, P = 0.6910; $F_{(1,52)}$ = 0.5729, P = 0.4530). Although not statistically significant, soils associated with *A. solidipes* had greater fungal richness and diversity, compared to *A. altimontana*. Bacterial richness measurements indicated that soils associated *Armillaria* species were slightly significant ($F_{(1,34)}$ = 3.905, P = 0.0563) with *A. altimontana* having greater richness. For both diversity indices, soils associated with *A. altimontana* had greater bacterial community diversity. Shannon's diversity was slightly significant ($F_{(1,34)}$ = 4.0619, P = 0.0518), though the Inverse Simpson index was not significant between *Armillaria* species ($F_{(1,34)}$ = 1.4005, P = 0.2448).

Additionally, *A. altimontana*, has a slightly significant positive relationship with fungal richness (P = 0.053; Supplemental Table 2). To analyze diversity measurements, the Shannon's diversity model was not significant (P = 0.489), while *A. altimontana* (P = 0.067; positive) and soil moisture (P = 0.078; negative) both had an influence on diversity. The ANOVA model for Inverse Simpsons was not significant (P = 0.558), as no variables were significant to the Inverse Simpson for fungal communities (Supplemental Table 2). Soil moisture had a significant negative relationship with bacterial richness (P = 0.013; Supplemental Table 3). Both *A. solidipes* (P = 0.039) and soil moisture (P = 0.022) had a significant negative relationship with bacterial Shannon's diversity. The bacterial Inverse Simpson diversity model

was significant (P = 0.0423), with soil moisture (P = 0.024, negative) as the lone significant predictor (Supplemental Table 3).

Bacterial and fungal beta diversity. Principal components analysis (PCoA) was completed to quantify beta diversity between bacterial and fungal communities associated with each *Armillaria* species. Beta diversity associated with soil bacterial communities of *A. altimontana* and *A. solidipes* were not significantly different (P = 0.544), and this is observed in the PCoA plot (Supplemental Figure 5). We also observed that beta diversity indices were significantly different for fungal soil communities associated with *Armillaria* species as well (P = 0.016) (Supplemental Figure 5).

Core communities associated with Armillaria **species.** Venn diagrams were constructed to identify the individual and core bacterial and fungal communities. Of the 6,677 total OTUs, the core bacterial communities for soils associated with both *Armillaria* species consisted of 955 OTUs (14.3%). While a significant abundance, 5,643 OTUs (84.5%), were uniquely associated with *A. altimontana*, only 79 (1.2%) were uniquely associated with *A. solidipes* (Figure 4b). The core fungal community associated with both *A. altimontana* and *A. solidipes* consisted of 521 OTUs (18.6%). Far surpassing the core community, 2,219 OTUs (79.1%) were unique to *A. altimontana*-associated soils, whereas only 66 (2.4%) OTUs were unique to *A. solidipes*-associated soils (Figure 4c).

Taxonomic trends and relative abundance. There were 17 16S bacterial families that exceeded the relative abundance of 1% (Figure 5A). All 17 families were in soils associated with *A. altimontana*. Pseudomonadadaceae was found in high abundance followed by Chthoniobacetaceae and Pyrinomonadaeae. Within the two soil bacterial communities associated with *A. solidipes*, we observed a large relative abundance of Entobacteriaceae, followed by Pseudomonadaceae (Figure 5A).

In total, 17 fungal families exceeded a relative abundance of 1% (Figure 5B). Mortierellaecea, Inocybaceae, Atheliaceae, Hypocreales, and Leotiomycetes were found in high relative abundance in soils associated with *A. altimontana*. Qualitatively, similar fungal families were observed in the three soil samples associated with *A. solidipes*, including Mortierellaceae, Leotiomycete, Inocybaceae, and Hypocreaceae, although at higher relatively abundance compared to *A. altimontana* (Figure 5B).

MetagenomeSeq analysis. We identified a total of four bacterial taxa that contributed significantly to the differential comparison between *Armillaria* species using the magnitude of OTU log-fold change (Figure 6A). A proliferation, at 90% confidence, of Nitrosococcaceae (wb1-P19), Solirubrobacteraceae, Enterobacteriaceae, and Gammoproteobacteria_PLTA13_fa were found in *A. solidipes*-associated soils; whereas, only uncultured bacteria were found to be significantly greater in *A. altimontana*-associated soils. We identified a total of five fungal taxa that contributed significantly to the comparison between *Armillaria* species using the magnitude of OTU log-fold change at the 90% confidence level (Figure 6B). These analyses identified a proliferation of Atheliaceae, Sulliaceae, Rhizopogonaeae, and unclassified

fungi in *A. altimontana*-associated soils; whereas only a single OTU (unclassified fungi) was significantly more abundant in *A. solidipes*-associated soils.

Discussion

We report the high-quality genome assemblies of two *Armillaria* species (*A. altimontana* and *A. solidipes*) that display different ecological behaviors, with structural and functional annotations. In addition, we examined the potential role and relationship among microbial communities that may correspond with the different ecological roles of *A. altimontana* and *A. solidipes*. *Armillaria* isolates were obtained from a conifer forest in northern Idaho within the interior western USA, where *A. altimontana* primarily behaves as a saprophyte and potentially beneficial biocontrol agent enhancing the growth/survival of western white pine [20] and *A. solidipes* primarily acts as an aggressive pathogen of diverse conifers [11, 13, 95]. In a whole-genome phylogenomic tree, *A. cepistipes* and *A. gallica*, which are often considered as weak or opportunistic pathogens, are closely related to *A. altimontana*. This result is similar to other published phylogenetic trees, where *A. altimontana* tends to group with less virulent pathogens (e.g., *A. cepistipes*, *A. calvescens*, *A. gallica*, and *A. nabsnona*) within the Gallica superclade, which is well separated from the *A. solidipes* group (e.g. *A. ostoyae*, *A. gemina*, and *A. sinapina*) within the Solidipes/Ostoyae superclade [22, 23; 96]. The phylogenetic placement of *A. altimontana*, compared to *A. mellea*, virulent pathogen within Mellea superclade, which is ancestral to the Gallica superclade, suggests that perhaps *A. altimontana* is evolving towards lower virulence.

The genome assemblies presented here were similar in size to other *Armillaria* genomes assemblies, although our *A. solidipes* genome is smaller than the *A. solidipes/ostoyae* 28-4 genome of Anderson and Spatafora (58.01 Mbp; JGI web site); this could be attributable to the different sequencing technologies used (PacBio and Illumina, respectively), and/or different isolates sequenced. Both *A. solidipes* assemblies are, however, smaller than the *A. ostoyae* C18/9 (60.1 Mbp) assembly from Europe [28]. Although it has been proposed that *A. solidipes* and *A. ostoyae* are a single species [97], genomic differences result in a separate grouping for *A. ostoyae* (C18/9) from Europe, which is distinct from the two *A. solidipes* isolates from North America in the whole genome phylogenetic tree. Thus, the phylogenomic analysis further supports that North American *A. solidipes* is distinct from Eurasian *A. ostoyae*.

Armillaria altimontana has a larger genome and a proportionately larger number of protein-coding genes compared to *A. solidipes*. It had twice as many sequences coding for repetitive elements (18,346,415 bp) than *A. solidipes* (9,691,790 bp); however, this difference is less than would be accounted for from the larger genome size alone (73.7 Mbp versus 55.7 Mbp, respectively). Rather, it has been suggested that gene family expansion has driven the increase of genome sizes in *Armillaria* in comparison with other Agaricales [28], and this could also be the mechanism responsible for the expanded genomes of *A. altimontana*, *A. cepistipes* (75.5 Mbp), and *A. gallica* (85.3 Mbp). Nevertheless, the genomes of *A.*

altimontana and *A. solidipes* shared large blocks of synteny (i.e., large blocks of gene order when comparing the two genomes) suggesting that their gene sets are similar within the genomes of two *Armillaria* species. Interestingly, *A. altimontana* genome encodes only slightly more secreted proteins, secreted CAZymes, ABC transporters, and secondary metabolite clusters, but with slightly fewer tRNA genes compared to *A. solidipes*; and it contains considerably more predicted non-secreted proteins.

Although relatively few genomic differences were observed, genome signatures of lifestyle differences between *A. solidipes* and *A. altimontana* were highlighted by the variation in putative secreted proteins. Approximately 1,200 encoded proteins in the two *Armillaria* genomes were found as potentially secreted, which could be potentially also considered as potential “effectors”- important proteins for interactions with a host [98]. Both species were well-equipped with genes encoding enzymes to degrade cell wall components, including cellulose, hemicellulose, lignin, pectin, proteins, and others. The major differences between the two *Armillaria* species are that *A. altimontana* had more carbohydrate-binding enzymes, beta-glucan- degrading enzymes, and more proteins with predicted to be involvement in host interactions (hydrophobin, cerato-platanin), especially small secreted proteins [99]. In contrast, the genome of *A. solidipes*, encoded more secreted putative cellulose, hemicellulose, pectin, and lignin-degrading enzymes. The combination of these secreted proteins could confer *A. solidipes* with a higher ability to infect and cause damage to its host. However, this hypothesis requires functional tests, because the number of CAZymes varies widely when comparing fungi with similar or different lifestyles [100]. Also, it has been found that phylogenetic history can have a more important influence on secretome composition than lifestyle [101].

We found that more than half of predicted proteins in *A. altimontana* and almost two thirds of *A. solidipes* predicted proteins could be considered orthologous. Most of these clusters had very similar numbers of proteins that were encoded in the genome of each *Armillaria* species. In contrast, all *A. altimontana* CBM67 proteins (15) were in a cluster, with only one CBM67 protein encoded by *A. solidipes*. Of the 15 *A. altimontana* CBM67 proteins, 11 were predicted as secreted, as was the one *A. solidipes* CBM67 protein. CBM67 is one of several CBM considered “lectin-like” and we speculate that in *Armillaria* spp. CBM67 proteins may have an additional functionality other that help in pectin degradation, such as interactions with the host and other organisms [102], particularly in *A. altimontana* which contains more CBM67 genes.

Among non-orthologous proteins, another major difference was observed in the total numbers of gene encoding cytochrome P450 enzymes: *A. altimontana* had considerably more both non-orthologous cytochrome P450 genes and a higher total of all cytochrome P450 genes, which are known to be involved in numerous metabolic pathways and biological processes including degradation of lignin and xenobiotics, secondary metabolite synthesis, and adaptation to different environments [88–91]. The versatile activities of cytochrome P450 enzymes makes it difficult to assign a specific function for them, but we speculate that a larger number of genes encoding these enzymes, including many non-orthologous enzymes, could be associated with different lifestyles, in this case more saprophytic/mycorrhizal lifestyle for *A. altimontana* and a more pathogenic lifestyle for *A. solidipes*. A

recent report also found a larger number of genes coding for cytochrome P450 in the saprophytic *A. cepistipes* compared to the pathogenic *A. ostoyae* [103].

Although non-orthologous proteins could have the similar molecular functions, their sequence differences could change their interactions with their substrates, or their regulation, or their environmental optima [104]. Furthermore, the expression levels and the timing of expression could account for important ecological differences in how the two *Armillaria* species interact with their hosts [103]. Variations in the expression of many genes, including some related to pathogenicity, have been observed even among strains of the same species, and these variations are associated with different levels of virulence during host infection [105].

Rhizomorphs are an important and unique means by which that *Armillaria* species interact with their environment, hosts, and substrates. Differences in microbial communities associated with each *Armillaria* species can perhaps be putatively attributed to genes encoding enzymes similar to those secondary metabolite synthesis enzymes previously identified in *Armillaria* species [28]. We observed some differences when comparing the number of genes upregulated in rhizomorphs in the two *Armillaria* species. For example, polyprenyl synthase genes involved in terpenoid synthesis were more abundant in *A. altimontana* compared to *A. solidipes*, whereas genes involved in the production of trichodiene, a potential signaling molecule or mycotoxin [106], were more abundant in *A. solidipes*. In general, terpenoids can have many different structures and functions, which have been involved in the interaction between fungi and plants and other organisms [107–110]. Trichodiene, on the other hand, is the immediate precursor to a family of toxins that cause damage to plant hosts [111].

Although overall differences of soil microbial communities were not observed in association with the two *Armillaria* species, several bacterial taxa were more abundant in soils associated with *A. solidipes*, and several fungal taxa were more abundant in association with *A. altimontana*. We identified the most significant logfold change of three Proteobacteria taxa within the Gammaproteobacteria class and Enterobacteriaceae in association with *A. solidipes*. Interestingly, one of these included Nitrosococcaceae wb1-P19, which is thought to be a nitrite-oxidizing autotrophic bacteria and that has previously been observed in caves [112–114]. In contrast, Gammaproteobacteria PLTA13_fa was found in high numbers in a Mn oxide-producing biofilm [115]. With these unique characteristics, it is not unexpected that some taxa within Proteobacteria have been characterized in soils contaminated with pesticides [116]. A recent study examining healthy ginseng and ginseng with rusty root also found that several Proteobacteria were found in high abundances among diseased plants [117], and increases in Proteobacteria were also observed in association with changes of cover types from forest to grasslands in Hawai'i [118]. In addition, Enterobacteriaceae taxa have been associated with higher levels of disease in Fusarium wilt disease of banana [119] but these taxa was found in higher levels in asymptomatic Kauri trees compared to those infected with *Phytophthora agathidicide* [120]. Similar to our study, however, Byers et al. [120] found that Solirubrobacterales were more abundant with trees in decline. Przemieniecki et al. [121] surveyed bacterial communities associated *A. ostoyae* rhizomorphs during three stages of tree decline. They observed that rhizomorphs that were rich in Parabacteriodes, Clostridium, and Bacillus were able to

hydrolyze diverse organic compounds that could assist *Armillaria* rhizomorph enzymes in wood decomposition. Though these taxa were not present in our study, the high abundance of several taxa in the Proteobacteria and Enterobacteriaceae may suggest recruitment of bacterial taxa by *A. solidipes* to assist in wood degradation. Alternatively, these results could suggest that the abundance of these taxa may be associated with tree mortality and/or changes in the plant community due to the activity of *A. solidipes*. Further, as the rhizosphere of the infected tree begins to degrade, these taxa may thrive because of their unique abilities to breakdown complex plant root materials. Several studies have observed changes in bacterial communities associated with declines in plant communities [122–124]. More research is needed better understand signaling among members of the pathobiome during tree decline drives changes in the associated bacterial communities

We identified several fungal taxa that were more abundant in association with *A. altimontana*. Several of these taxa have been shown to increase plant productivity through multiple functions, such as ectomycorrhizal fungi including Atheliaceae, Rhizopogonaceae, and Suillaceae [125–128]. Taxa from all three ectomycorrhizal fungal families were significantly more abundant in soils associated with *A. altimontana* compared to *A. solidipes*, and these taxa are perhaps ectomycorrhizal, allowing increased uptake of water and nutrients to enhance tree defenses against root diseases [31]. The functions of these *A. altimontana*-associated, soil fungi suggest that these fungal communities may also contribute to the overall health of the forest stand, corroborating Warwell et al. [20], who found that trees associated with *A. altimontana* were larger in both diameter and height than trees not associated with this *Armillaria* species. It remains unknown if *A. altimontana* is conducive to mycorrhizal fungi though evidence provided herein suggests that *A. altimontana* co-occurs with mycorrhizal fungi.

Utilizing the natural soil fungal communities to assist in the management of Armillaria root disease may be key to long-term protection of residual trees on sites infested with pathogenic *Armillaria* spp., such as following Armillaria root disease-associated mortality or silvicultural thinning practices. Beneficial microbes can minimize pathogen inoculum loads by reducing pathogen growth or inhibiting pathogen infection of susceptible hosts [41]. In this study, a greater diversity of mycorrhizal and saprophytic fungi was observed in association with the beneficial/non-pathogenic *A. altimontana*, demonstrating that mycorrhizae may have a direct influence on hosts within forested environments associated with *Armillaria* species [125].

Selecting trees to sample *Armillaria* species was the greatest limiting factor in this study. More than 25 years before this study, *A. solidipes* was well represented on the site [20]. The small number of *A. solidipes*-infected trees in this study perhaps reflects the protective role of *A. altimontana* and the associated microbial community in suppressing *A. solidipes*; however, additional studies and surveys are needed to support this hypothesis. The survey approaches used in our study yielded rhizomorphs for 78% of the trees and adequate DNA from 90% of the samples. Additionally, the use of metatranscriptomics could further our understanding of the fungal microbes and their ecological functions within the soils associated with *A. altimontana* and *A. solidipes*.

In conclusion, we found high similarity comparing the genomes of between the beneficial/non-pathogenic *A. altimontana* and pathogenic *A. solidipes*. The larger number of proteins encoded within *A. altimontana* genome results from moderate increases across many different gene families instead of a large expansion of a few gene families. However, we found many relatively small differences in genes that could contribute to differences in ecological lifestyles and interactions with woody hosts and soil microbes (fungi and bacteria). We did observe, however, that soil microbial communities may act in concert with *A. altimontana* to produce suppressive soils that help protect trees from Armillaria root disease, caused by *A. solidipes*. This study further suggests that novel approaches for managing Armillaria root disease could be based on management practices that favor naturally occurring, non-pathogenic *Armillaria* spp. and other beneficial soil microbes that suppress Armillaria root disease. Additionally, continued observations of microbial communities in association *Armillaria* spp. will provide additional insights on microbial changes over time in relation with Armillaria root disease and changing forest environments.

Declarations

Acknowledgments

We thank the USDA Forest Service, State & Private forestry, Forest Health Protection, Special Technology Development Program and Joint Venture Agreements (19-JV-11221633-093 and 20-JV-11221633-141) to Colorado State University (JES) for partial funding of this study.

Author contributions: All authors contributed to the study conception and design. Material preparation and data collection were performed by Bradley Lalande, John Hanna, Mee-Sook Kim, Ned Klopfenstein and Jane Stewart. Analyses were performed by Jorge Ibarra Caballero, Bradley Lalande, and Jane Stewart. The first draft of the manuscript was written by Jorge Ibarra Caballero, Bradley Lalande and Jane Stewart, and all authors commented on previous versions of the manuscript. All authors read and approved the final manuscript.

Conflict of Interest: The authors declare that they have no conflict of interest.

Compliance with ethical standards: For this type of study formal consent is not required.

Funding: This study was funded in part by the USDA Forest Service, State & Private forestry, Forest Health Protection, Special Technology Development Program and Joint Venture Agreements (19-JV-11221633-093 and 20-JV-11221633-141) to Colorado State University (JES).

Data availability: The datasets generated during and/or analysed during the current study are available in the NCBI database. The corresponding genome assemblies were deposited at the NCBI with accession number JAIWYR000000000 for *A. altimontana*, and JAIWYQ000000000 for *A. solidipes*, and microbial dataset is in NCBI SRA database under accession number PRJNA767898.

References

1. Hess J, Skrede I, Chaib De Mares M, Hainaut M, Henrissat B, Pringle A (2018) Rapid divergence of genome architectures following the origin of an ectomycorrhizal symbiosis in the gene Amanita. Molecular Biology and Evolution. 35:2786-2804. doi.org/10.1093/molbev/msy179.
2. Möller M, Stukenbrock EH (2017) Evolution and genome architecture in fungal plant pathogens. Nature Reviews Microbiology. 15:756-771. DOI: 10.1038/nrmicro.2017.76.
3. Ryberg M, Matheny PB (2012) Asynchronous origins of ectomycorrhial clades of Agaricales. Proceedings of the Royal Society B. 279:2003-2011. doi.org/10.1098/rspb.2011.2428.
4. Tedersoo L, May TW, Smith ME (2010). Ectomycorrhizal lifestyle in fungi: global diversity, distribution, and evolution of phylogenetic lineages. Mycorrhiza. 20:217-263. doi: 10.1007/s00572-009-0274-x.
5. Kohler A, Kuo A, Nagy L. *et al.* (2015) Convergent losses of decay mechanisms and rapid turnover of symbiosis genes in mycorrhizal mutualists. Nature Genetics. 47:410–415. doi.org/10.1038/ng.3223.
6. Veneault-Fourrey C, Commun C, Kohler A, Morin E, Balestrini R, Plett J, Danchin E, Coutinho P, Wiebenga A, DeVries RP, Henrissat B, Martin F (2014) Genomic and transcriptomic analysis of *Laccaria bicolor* CAZome reveals insights into polysaccharides remodelling during symbiosis establishment. Fungal Genetics and Biology. 72:168-181. doi: 10.1016/j.fgb.2014.08.007.
7. Dalman K, Himmelstrand K, Olson A, Lind M, Brandstörm-During M, Stenlid J (2013) A genome-wide association study identifies genomic regions for virulence in the non-model organism *Heterobasidion annosum* s.s. PLoSOne. 8:e53525. doi: 10.1371/journal.pone.0053525.
8. Zeng Z, Sun H, Vainio EJ, Raffaello T, Kovalchuk A, Morin E, Duplessis S, Asiegbu FO (2018) Intraspecific comparative genomics of isolates of the Norway spruce pathogen (*Heterobaidion parviporum*) and identification of its potential virulence factors. BMC Genomics. 19:220. doi.org/10.1186/s12864-018-4610-4.
9. Castanera R, Borgognone A, Pisbarro AG, Ramírez L (2017) Biology, dynamics and applications of transposable elements in basidiomycete fungi. Applied Microbiology and Biotechnology. 101: 1337-1350. DOI 10.1007/s00253-017-8097-8.
10. Marçais B, Bréda N (2006) Role of an opportunistic pathogen in the decline of stressed oak trees. Journal of Ecology. 94:1214-1223. doi.org/10.1111/j.1365-2745.2006.01173.x.
11. Baumgartner K, Coetzee MPA, Hoffmeister D (2011) Secrets of the subterranean pathosystem of *Armillaria*. Molecular Plant Pathology. 12:515-534. doi.org/10.1111/j.1364-3703.2010.00693.x.
12. Cleary MR, van der Kamp BJ, Morrison DJ (2012) Pathogenicity and virulence of *Armillaria sinapina* and host response to infection in Douglas-fir, western hemlock and western redcedar in the southern Interior of British Columbia. Forest Pathology. 42:481-491. https://doi.org/10.1111/j.1439-0329.2012.00782.x.
13. Heinzelmann R, Prospero S, Rigling D (2017) Virulence and Stump Colonization Ability of *Armillaria borealis* on Norway Spruce Seedlings in Comparison to Sympatric *Armillaria* species. Plant Disease.

101:470-479. doi.org/10.1094/PDIS-06-16-0933-RE.

14. Morrison DJ, Pellow KW (2002) Variation in virulence among isolates of *Armillaria ostoyae*. Forest Pathology. 32:99-107. DOI: 10.1046/j.1439-0329.2002.00275.x.
15. Morrison DJ (2004) Rhizomorph growth habit, saprophytic ability and virulence of 15 *Armillaria* species. Forest Pathology 34:15-26. DOI: 10.1046/j.1439-0329.2003.00345.x.
16. Prospero S, Holdenrieder O, Rigling D (2004) Comparison of the virulence of *Armillaria cepistipes* and *Armillaria ostoyae* on four Norway spruce provenances. Forest Pathology. 34:1-14. doi.org/10.1046/j.1437-4781.2003.00339.x.
17. Brazee NJ, Ortiz-Santana B, Banik MT, Lindner DL (2012) *Armillaria altimontana*, a new species from the western interior of North America. Mycologia. 104(5):1200-1205. DOI: 10.3852/11-409.
18. Ferguson BA, Dreisbach TA, Parks CG, Filip G, Schmitt CL (2003) Coarse-scale population structure of pathogenic *Armillaria* species in a mixed conifer forest in the Blue Mountains of northeast Oregon. Canadian Journal of Forest Research. 33:612–633. DOI: 10.1139/x03-065.
19. Kim M-S, Klopfenstein NB, McDonald GI, Arumuganathan K, Vidaver AK (2000) Characterization of North America *Armillaria* Species by Nuclear DNA Content and RFLP Analysis. Mycologia. 92:874-883. doi.org/10.1080/00275514.2000.12061232.
20. Warwell MV, McDonald GI, Hanna JW, Kim MS, Lalande BM, Stewart JE, Hudak AT, Klopfenstein NB (2019) *Armillaria altimontana* is associated with healthy western white pine (*Pinus monticola*): Potential *in situ* biological control of Armillaria root disease pathogen, *A. solidipes.* Forests.10:294. DOI: https://doi.org/10.3390/f10040294.
21. Rizzo DM, Harrington TC (1993) Delineation and biology of clones of *Armillaria ostoyae*, *A. gemina* and *A. calvescens*. Mycologia, 85(2):164-174. doi.org/10.2307/3760452.
22. Klopfenstein NB, Stewart JE, Ota Y, Hanna JW, Richardson BA, Ross-Davis AL, Elías-Román RD, Korhonen K, Keča N, Iturritxa E, Alvarado-Rosales D, Solheim H, Brazee NJ, Łakomy P, Cleary MR, Hasegawa E, Kikuchi T, Garza-Ocañas F, Tsopelas P, Rigling D, Prospero S, Tsykun T, Bérubé JA, Stefani FOP, Jafarpour S, Antonín V, Tomšovský M, McDonald GI, Woodward S, Kim MS (2017) Insights into the phylogeny of Northern Hemisphere Armillaria: Neighbor-net and Bayesian analyses of translation elongation factor 1-α gene sequences. Mycologia. 109:75-91. doi.org/10.1080/00275514.2017.1286572.
23. Koch RA, Wilson AW, Séné O, Henkel TW, Aime MC (2017) Resolved phylogeny and biogeography of the root pathogen Armillaria and its gasteroid relative, *Guyanagaster*. BMC Evolutionary Biology. 17:33-48. doi.org/10.1186/s12862-017-0877-3.
24. Heinzelmann R, Dutech C, Tsykun T, Labbé F, Soularue J-P, Prospero S (2019) Latest advances and future perspectives in *Armillaria* research. Canadian Journal of Plant Pathology. 41:1–23. doi.org/10.1080/07060661.2018.1558284.
25. Devkota P, Hammerschmidt R (2020) The infection process of *Armillaria mellea* and *Armillaria solidipes*. Physiological and Molecular Plant Pathology. 112:101543. DOI:10.1016/j.pmpp.2020.101543.

26. Collins C, Keane TM, Turner DJ, O'Keefe G, Fitzpatrick DA, Doyle, S (2013) Genomic and Proteomic Dissection of the Ubiquitous Plant Pathogen, *Armillaria mellea*: Toward a New Infection Model System. Journal of Proteome Research. 12:2552-2570. doi: 10.1021/pr301131t.
27. Ross-Davis AL, Stewart JE, Hanna JW, Kim M-S, Cronn R, Rai H, Richardson BR, McDonald GI, Klopfenstein NB (2013)Transcriptome characterization of an Armillaria root disease pathogen reveals candidate pathogenicity-related genes.Forest Pathology. 43:468-477. DOI: 10.1111/efp.12056.
28. Sipos G, Prasanna AN, Walter MC, O'Connor E, Bálint B, Krizsán K, Kiss B, Hess J, Varga T, Slot J, Riley R, Bóka B, Rigling D, Barry K, Lee J, Mihaltcheva S, LaButti K, Lipzen A, Waldron R, Moloney NM, Sperisen C, Kredics L, Vágvölgyi C, Patrignani A, Fitzpatrick D, Nagy I, Doyle S, Anderson JB, Grigoriev IV, Güldener U, Münsterkötter M, Nagy LG (2017) Genome expansion and lineage-specific genetic innovations in the forest pathogenic fungi *Armillaria*. Nature Ecology and Evolution 1:1931-1941. doi.org/10.1038/s41559-017-0347-8.
29. Azul AM, Nunes J, Ferreira I, Coehlo AS, Verissmo P, Trovao J, Campos A, Castro O, Freitas H (2014) Valuing native ectomycorrhizal fungi as a Mediterranean forestry component for sustainable and innovative solutions. Botany. 92:161-171. dx.doi.org/10.1139/cjb-2013-0170.
30. Baldrian P (2017) Forest microbiome: Diversity, complexity, and dynamics. *FEMS* Microbiology. 42:109-130. doi.org/10.1093/femsre/fuw040.
31. Leake J, Johnson D, Donnelly D, Muckle G, Boddy L, Read D (2004) Networks of power and influence: The role of mycorrhizal mycelium in controlling plant communities and agroecosystem functioning. Canadian Journal of Botany. 82:1016-1045. doi.org/10.1139/b04-060.
32. Lee Taylor D, Sinsabaugh RL (2014) Chapter 4: The soil fungi: Occurrence, phylogeny, and ecology. In E.A. Paul (4th ed.), *Soil microbiology, ecology and biochemistry*. Cambridge, MA: Academic Press. p. 339-382. eBook ISBN: 9780123914118. https://doi.org/10.1016/C2011-0-05497-2.
33. Saif SR, Khan AG (1975) The influence of season and stage of development of plant on endogone mycorrhiza of field-grown wheat. Canadian Journal of Microbiology. 82:1020–1024. DOI: 10.1139/m75-151.
34. Cardenas E, Kranabetter JM, Hope G, Maas KR, Hallam S, Mohn WM (2015) Forest harvesting reduces the soil metagenomic potential for biomass decomposition. ISME. 9: 2465-2476. DOI: 10.1038/ismej.2015.57.
35. Chapman SK, Koch GW (2007) What type of diversity yields synergy during mixed litter decomposition in a natural forest ecosystem? Plant Soil. 299: 153-162. 10.1007/s11104-007-9372-8.
36. Davidson EA, Janssens IA (2006) Temperature sensitivity of soil carbon decomposition and feedbacks to climate change. Nature. 440:165-173. doi.org/10.1038/nature04514.
37. Robertson GP, Groffman PM (2014) Chapter 14: Nitrogen transformation. In E.A. Paul (4th ed.), *Soil microbiology, ecology and biochemistry*. Cambridge, MA: Academic Press. p. 339-382. eBook ISBN: 9780123914118. https://doi.org/10.1016/C2011-0-05497-2.

38. Schloter M, Dilly O, Munch JC (2003) Indicators for evaluating soil quality. Agriculture, Ecosystems, and Environment. 98:255-262. doi.org/10.1016/S0167-8809(03)00085-9.

39. Allison SD, Martiny JBH (2008) Resistance, resilience, and redundancy in microbial communities. PNAS. 105(1):11512-11519. doi.org/10.1073/pnas.0801925105.

40. Horwath W (2014) Chapter 12: Carbon cycling: The dynamics and formation of organic matter. In E.A. Paul (4th ed.), *Soil microbiology, ecology and biochemistry*. Cambridge, MA: Academic Press. p. 339-382. eBook ISBN: 9780123914118. https://doi.org/10.1016/C2011-0-05497-2.

41. Kile GA, McDonald GI, Byler JW (1991) Ecology and disease in natural forests. In: C.G. Shaw and G.A. Kile, Armillaria Root Disease. United States Department of Agriculture Forest Service. Agricultural Handbook No. 691. Washington D.C. p. 102-121.

42. Kim MS, Ross-Davis AL, Stewart JE, Hanna JW, Warwell MV, Zambino PJ, Cleaver C, McDonald GI, Page-Dumroese DS, Moltzan B, Klopfenstein NB (2016) Can metagenomic studies of soil microbial communities provide novel insights toward developing novel management approaches for Armillaria root disease? Ramsey, A. and Palacios, P., compilers. Proceedings of the 63rd annual Western International Forest Disease Work Conference, Sept. 21-25, 2015. Newport, OR, USA.

43. Stewart JE, Kim M-S, Lalande, BM, Klopfenstein NB (2021) Pathobiome and microbial communities associated with forest tree root diseases [Chapter 15]. In: Asiegbu, Fred O.; Kovalchuk, Andriy, eds. Forest Microbiology - Tree Microbiome: Phyllosphere, Endosphere, and Rhizosphere, Volume 1. London, UK: Academic Press, Elsevier, Inc. p. 277-292. https://doi.org/10.1016/C2019-0-03562-5.

44. Kedves O, Shahab D, Champramary S, Chen L, Indic G, Bóka B, Nagy VD, Vágvölgyi C, Kredics L, Sipos G (2021) Epidemiology, biotic interactions, and biological control of Armillarioids in the Northern Hemisphere. Pathogens. 10:76. doi.org/10.3390/pathogens10010076.

45. Ross-Davis A, Settles M, Hanna JW, Shaw JD, Hudak AT, Page-Dumroese DS, Klopfenstein NB (2015) Using a metagenomic approach to improve our understanding of Armillaria root disease. pp. 73-78 in: Murray, M. and Palacios, P., compilers. Proceedings of the 62nd annual Western International Forest Disease Work Conference, Sept. 8-12, 2014. Cedar City, UT, USA.

46. Gurevich A, Saveliev V, Vyahhi N, Tesler G (2013) QUAST: quality assessment tool for genome assemblies. Bioinformatics. 29(8):1072-1075. doi: 10.1093/bioinformatics/btt086.

47. Simão FA, Waterhouse RM, Ioannidis P, Kriventseva EV, Zdobnov EM (2015) BUSCO: assessing genome assembly and annotation completeness with single-copy orthologs. Bioinformatics 31(19):3210-3212. doi.org/10.1093/bioinformatics/btv351.

48. Bertels F, Silander OK, Pachkov M, Rainey PB, van Nimwegen E (2014) Automated reconstruction of whole genome phylogenies from short sequence reads. Molecular Biology and Evolution. 31(5):1077-1088. DOI: 10.1093/molbev/msu088.

49. Langmead, B. and Salzberg, S.L. 2012. Fast gapped-read alignment with Bowtie 2. Nature Methods 9:357–359. doi: 10.1038/nmeth.1923.

50. Guindon S, Dufayard JF, Lefort V, Anisimova M, Hordijk W, Gascuel O (2010) New Algorithms and Methods to Estimate Maximum-Likelihood Phylogenies: Assessing the Performance of PhyML 3.0.

Systematic Biology. 59(3):307-21. doi.org/10.1093/sysbio/syq010.

51. Smit AFA, Hubley R (2015) RepeatModeler Open-1.0. 2013—2015. Available from: www.repeatmasker.org.
52. Cantarel BL, Korf I, Robb SMC, Parra G, Ross E, Moore B, Holt C, Sánchez Alvarado A, Yandell M (2008) MAKER: An easy-to-use annotation pipeline designed for emerging model organism genomes. Genome Research 18(1):188-196. DOI: 10.1101/gr.6743907
53. Smit AR, Hubley R, Green P (2013) RepeatMasker Open-4.0. http:// www.repeatmasker.org.
54. Keller O, Kollmar M, Stanke M, Waack S (2011) A novel hybrid gene prediction method employing protein multiple sequence alignments. Bioinformatics 27(6):757-763. doi: 10.1093/bioinformatics/btr010.
55. Ter-Hovhannisyan V, Lomsadze A, Chernoff Y, Borodovsky M (2008) Gene prediction in novel fungal genomes using an ab initio algorithm with unsupervised training. Genome Research 18:1979-1990. doi: 10.1101/gr.081612.108.
56. Zaharia M, Bolosky WJ, Curtis K, Fox A, Patterson D, Shenker S, Stoica I, Karp RM, Sittler T (2011) Faster and More Accurate Sequence Alignment with SNAP. arXiv:1111.5572v1.
57. Lowe TM, Eddy SR (1997) tRNAscan-SE: a program for improved detection of transfer RNA genes in genomic sequence. Nucleic Acids Research 25:955–964. PMCID: PMC146525. DOI: 10.1093/nar/25.5.955.
58. Camacho C, Coulouris G, Avagyan V, Ma N, Papadopoulos J, Bealer K, Madden TL (2009) BLAST+: architecture and applications. BMC Bioinformatics 10:421-429. doi.org/10.1186/1471-2105-10-421.
59. Jones P, Binns D, Chang H, Fraser M, Li W, McAnulla C, McWilliam H, Maslen J, Mitchell A, Nuka G, Pesseat S, Quinn AF, Sangrador-Vegas A, Scheremetjew M, Yong S, Lopez R, Hunter S. 2014. InterProScan 5: genome-scale protein function classification. Bioinformatics. 30(9):1236-40. doi: 10.1093/bioinformatics/btu031.
60. Zhang H, Yohe T, Huang L, Entwistle S, Wu P, Yang Z, Busk PK, Xu Y, Yin Y (2018) dbCAN2: a meta server for automated carbohydrate-active enzyme annotation. Nucleic Acids Research 46:W95-W101. DOI: 10.1093/nar/gky418.
61. Urban M, Cuzick A, Seager J, Wood V, Rutherford K, Venkatesh SY, De Silva N, Martinez MC, Pedro H, Yates AD, Hassani-Pak K, Hammond-Kosack KE (2020) PHI-base: the pathogen–host interactions database. Nucleic Acids Research. 48: D613–D620. https://doi.org/10.1093/nar/gkz904.
62. Blin K, Shaw S, Steinke K, Villebro R, Ziemert N, Lee SY, Medema MH, Weber T (2019) antiSMASH 5.0: updates to the secondary metabolite genome mining pipeline. *Nucleic Acids Research*. Volume 47, Issue W1:W81–W87. doi.org/10.1093/nar/gkz310.
63. Almagro Armenteros JJ, Sønderby CK, Sønderby SK, Nielsen H, Winther O (2017) DeepLoc: prediction of protein subcellular localization using deep learning. *Bioinformatics*. 33:3387–3395. doi: 10.1093/bioinformatics/btx431.
64. Soderlund C, Nelson W, Shoemaker A, Paterson A (2006) SyMAP: A System for Discovering and Viewing Syntenic Regions of FPC maps. Genome Research 16:1159-1168. DOI: 10.1101/gr.5396706.

65. Soderlund C, Bomhoff M, Nelson W (2011) SyMAP: A turnkey synteny system with application to plant genomes. Nucleic Acids Research 39(10):e68. doi.org/10.1093/nar/gkr123.
66. Xu L, Dong Z, Fang L, Luo Y, Wei Z, Guo H, Zhang G, Gu YQ, Coleman-Derr D, Xia Q, Wang Y (2019) OrthoVenn2: a web server for whole-genome comparison and annotation of orthologous clusters across multiple species. *Nucleic Acids Research*. 47:W52–W58. DOI: 10.1093/nar/gkz333.
67. Rehner SA, Buckley E. 2005. A Beauveria phylogeny inferred from nuclear ITS and EF1-a sequences: evidence for cryptic diversification and links to Cordyceps teleomorphs. Mycologia. 97:84–98. DOI: 10.3852/mycologia.97.1.84
68. White TJ, Bruns T, Taylor J (1990) Amplification and direct sequencing of fungal ribosomal RNA genes for phylognetics. In: *A Guide to Molecular Methods and Applications* (Innis MA, Gelfand DH, Sninsky JJ, White JW, eds). Academic Press, New York: 315–322. dx.doi.org/10.1016/B978-0-12-372180-8.50042-1.
69. Walters W, Hyde ER, Berg-Lyons D, Ackermann G, Humphrey G, Parada A, Gilbert JA, Jansson JK, Caporaso JG, Fuhrman JA, Apprill A, Knight B (2015) Improved bacterial 16S rRNA gene (V4 and V4-5) and fungal internal transcribed spacer marker gene primers for microbial community surveys. mSystems 1(1):e00009-15. doi: 10.1128/mSystems.00009-15.
70. Bolger AM, Lohse M, Usadel B (2014) Trimmomatic: A flexible trimmer for Illumina Sequence Data. Bioinformatics. 30:2114-2120. doi.org/10.1093/bioinformatics/btu170
71. Schloss PD, Westcott SL, Ryabin T, Hall JR, Hartmann M, Hollister EB, Lesniewski RA, Oakley BB, Parks DH, Robinson CJ, Sahl JW, Stres B, Thallinger GG, Van Horn DJ, Weber CF (2009) Introducing mothur: Open-source, platform-independent, community-supported software for describing and comparing microbial communities. Applied and Environmental Microbiology. 75:7537-7541. dx.doi.org/10.1128/AEM.01541-09.
72. Kozich JJ, Westcott SL, Baxter NT, Highlander SK, Schloss PD (2013) Development of a Dual-Index Sequencing Strategy and Curation Pipeline for Analyzing Amplicon Sequence Data on the MiSeq Illumina Sequencing Platform. Applied and Environmental Microbiology. 79:5112–5120. doi:10.1128/AEM.01043-13.
73. Edgar RC, Haas BJ, Clemente JC, Quince C, Knight R (2011) UCHIME improves sensitivity and speed of chimera detection. Bioinformatics. 27:2194-200. doi.org/10.1093/bioinformatics/btr381.
74. Edgar RC (2010) Search and clustering orders of magnitude faster than BLAST. *Bioinformatics*. 26(19):2460–2461. https://doi.org/10.1093/bioinformatics/btq461.
75. Quast C, Pruesse E, Yilmaz P, Gerken J, Schweer T, Yarza P, Peplies J, Glöckner FO (2013) **The SILVA ribosomal RNA gene database project: improved data processing and web-based tools**. Nucleic Acid Res.41:D590-D596. DOI: 10.1093/nar/gks1219.
76. Nilsson RH, Larsson K-H, Taylor AFS, Bengtsson-Palme J, Jeppesen JS, Schigel D, Kennedy P, Picard K, Glöckner FO, Tedersoo L, Saar I, Kõljalg U, Abarenkov K (2019) The UNITE database for molecular identification of fungi: handling dark taxa and parallel taxonomic classifications. *Nucleic Acids Research*. 47:D259–D264. doi: 10.1093/nar/gky1022.

77. Wang Q, Garrity GM, Tiedje JM, Cole JR (2007) Naïve Bayesian classifier for rapid assignment of rRNA sequences into the new bacterial taxonomy. Applied and Environmental Microbiology. 73: 5261-5267. DOI: 10.1128/AEM.00062-07.

78. Oksanen J, Blanchet FG, Friendly M, Kindt R, Legendre P, McGlinn D, Minchin PR, O'Hara RB, Simpson GL, Solymos P, Stevens MHH, Szoecs E, Wagner H (2017) vegan: Community Ecology Package. R package version 2.4-2.

79. Olofsson TC, Vásquez A (2008) **Detection and identification of a novel lactic acid bacterial flora within the honey stomach of the honeybee***Apis mellifera.* Current Microbiology. 57:356-363. DOI: 10.1007/s00284-008-9202-0.

80. Hill TCJ, Walsh KA, Harris JA, Moffett BF (2006) Using ecological diversity measures with bacterial communities. FEMS Microbiology Ecology. 43:1-11. doi.org/10.1111/j.1574-6941.2003.tb01040.x.

81. Nagendra H (2002) Opposite trends in response to Shannon and Simpson indices of landscape diversity. Applied Geography. 22:175-186. dx.doi.org/10.1016/S0143-6228(02)00002-4.

82. Zhang H, John R, Peng Z, Yuan J, Chu C, Du G, Zhou S (2012) The relationship between species richness and evenness in plant communities along a successional gradient: A study from sub-alpine meadows of the eastern Qinghai-Tibetan Plateau, China. PLoS ONE 7:e49024. DOI: 10.1371/journal.pone.0049024.

83. Paulson JN, Talukder H, Pop M, Bravo HC (2021) metagenomeSeq: Statistical analysis for sparse high-throughput sequencing. Bioconductor package: 1.16.0.

84. Wickham H (2016) *ggplot2: Elegant Graphics for Data Analysis*. Springer-Verlag New York. ISBN 978-3-319-24277-4. https://ggplot2.tidyverse.org.

85. Santana MF, Queiroz MV (2015) Transposable Elements in Fungi: A Genomic Approach. Scientific Journal of Genetics and Gene Therapy 1(1):012-016.

86. Coleman JJ, Mylonakis E (2009) Efflux in Fungi: La Pièce de Résistance. PLoS Pathogens 5(6): e1000486. https://doi.org/10.1371/journal.ppat.1000486.

87. Macheleidt J, Mattern DJ, Fischer J, Netzker T, Weber J, Schroeckh V, Valiantem V, Brakhage AA (2016) Regulation and Role of Fungal Secondary Metabolites. Annual Review of Genetics 50:371-392. DOI: 10.1146/annurev-genet-120215-035203.

88. Syed K, Yadav JS (2012) P450monooxygenases (P450ome) of the model white rot fungus *Phanerochaete chrysosporium*. Critical Reviews in Microbiology 38(4):339-363. doi: 10.3109/1040841X.2012.682050.

89. Ichinose H (2013) Cytochrome P450 of wood-rotting basidiomycetes and biotechnological applications. Biotechnology and Applied Biochemistry. 60:71-81. DOI: 10.1002/bab.1061.

90. Qhanya LB, Matowane G, Chen W, Sun Y, Letsimo EM, Parvez M, Yu J-H, Mashele SS, Syed K (2015) Genome-Wide Annotation and Comparative Analysis of Cytochrome P450 Monooxygenases in Basidiomycete Biotrophic Plant Pathogens. PLOS ONE. 10(11):e0142100. doi.org/10.1371/journal.pone.0142100.

91. Durairaj P, Hur J-S, Yun H (2016) Versatile biocatalysis of fungal cytochrome P450 monoxygenases. Microbial Cell Factories. 15:125. doi.org/10.1186/s12934-016-0523-6.
92. Gonçalves AP, Heller J, Daskalov A, Videra A, Glass NL (2017) Regulated forms of cell death in fungi. Frontiers in Microbiology 8:1837. doi.org/10.3389/fmicb.2017.01837.
93. Schmidt-Dannert C (2014) Biosynthesis of terpenoid natural products in fungi. In: Schrader J., Bohlmann J. (eds) *Biotechnology of Isoprenoids. Advances in Biochemical Engineering/Biotechnology*, vol 148. Springer, Cham. DOI: 10.1007/10_2014_283.
94. Quin MB, Flynn CM, Schmidt-Dannert C (2014) Traversing the fungal terpenome. Natural Product Reports 31(10):1449-1473. doi: 10.1039/c4np00075g.
95. Shaw CG III, Roth L (1978). Control of Armillaria root rot in managed coniferous forests. European Journal of Forest Pathology. 8:163-174. doi.org/10.1111/j.1439-0329.1978.tb01463.x.
96. Coetzee MPA, Wingfield BD, Wingfield MJ (2018) Armillaria root-rot pathogens: Species boundaries and global distribution. MDPI Pathogens 7:83. https://doi.org/10.3390/pathogens7040083
97. Burdsall HH, Volk, TJ (2008) *Armillaria solidipes*, an older name for the fungus called *Armillaria ostoyae*. North American Fungi. 3:261–267. DOI: http://dx.doi.org/10.2509/naf2008.003.00717.
98. Presti LL, Lanver D, Schweizer G, Tanaka S, Liang L, Tollot M, Zuccaro A, Reissmann S, Kahmann R (2015) Fungal effectors and plant susceptibility. Annual Review of Plant Biology 66:513-545. doi.org/10.1146/annurev-arplant-043014-114623.
99. Kim K, Jeon J, Choi J, Cheong K, Song H, Choi G, Kang S, Lee Y (2016) Kingdom-wide analysis of fungal small secreted proteins (SSPs) reveals their potential role in host association. Frontiers in Plant Science. 7:186. doi: 10.3389/fpls.2016.00186.
100. Zhao Z, Liu H, Wang C, Xu J-R (2013) Comparative analysis of fungal genomes reveals different plant cell wall degrading capacity in fungi. BMC Genomics 14:274-288. doi.org/10.1186/1471-2164-14-274.
101. Krijger J-J, Thon MR, Deising HB, Wirsel SGR (2014) Compositions of fungal secretomes indicate a greater impact of phylogenetic history than lifestyle adaptation. BMC Genomics 15:722-739. doi.org/10.1186/1471-2164-15-722.
102. Varrot A, Basheer SM, Imberty A (2013) Fungal lectins: structure, function and potential applications. Current Opinion in Structural Biology 23:678-685. http://dx.doi.org/10.1016/j.sbi.2013.07.007 .
103. Sahu N, Merényi Z, Bálint B, Kiss B, Sipos G, Owens R, Nagy LG (2020) Hallmarks of basidiomycete soft- and white-rot in wood-decay-omics data of Armillaria. bioRxiv 2020.05.04.075879; doi.org/10.1101/2020.05.04.075879.
104. Neuwald AF, Aravind L, Altschul SF (2018) Inferring joint sequence-structural determinants of protein functional specificity. eLIFE 7:e29880. doi.org/10.7554/eLife.29880.001.
105. Palma-Guerrero J, Ma X, Torriani SFF, Zala M, Francisco CS, Hartmann FE, Croll D, McDonald BA (2017) Comparative Transcriptome Analyses in Zymoseptoria tritici Reveal Significant Differences in Gene Expression Among Strains During Plant Infection. Molecular Plant-Microbe Interactions. 30:231-244. doi.org/10.1094/MPMI-07-16-0146-R.

106. Kimura M, Takai T, Takahashi-Ando N, Ahsato S, Fujimura M (2007) Molecular and genetic studies of *Fusarium* trichothecene biosynthesis: pathoways, genes, and evolution. Bioscience, Biotechnology, and Biochemistry. 71:1-19. DOI: 10.1271/bbb.70183.

107. Schmidt R, Etalo DW, de Jager V, Gerards S, Zweers H, de Boer W, Garbeva P (2016) Microbial Small Talk: Volatiles in Fungal–Bacterial Interactions. Frontiers in Microbiology 6:1495. doi.org/10.3389/fmicb.2015.01495.

108. Deveau A, Bonito G, Uehling J, Paoletti M, Becker M, Bindschedler S, Hacquard S, Hervé V, Labbé J, Lastovetsky OA, Mieszkin S, Millet LJ, Vajna B, Junier P, Bonfante P, Krom BP, Olsson S, Dirk van Elsas J, Wick, LY (2018) Bacterial–fungal interactions: ecology, mechanisms and challenges. *FEMS Microbiology Reviews*. 42:335–352. doi: 10.1093/femsre/fuy008.

109. Huang AC, Osbourn A (2019) Plant terpenes that mediate below-ground interactions: prospects for bioengineering terpenoids for plant protection. Pest Management Science. 75:2368-2377. doi: 10.1002/ps.5410.

110. Farh ME, Jeon J (2020) Roles of fungal volatiles from perspective of distinct lifestyles in filamentous fungi. The Plant Pathology Journal. 36:193-203. doi:10.5423/PPJ.RW.02.2020.0025.

111. Proctor RH, McCormick SP, Kim H, Cardoza RE, Stanley AM, Lindo L, Kelly A, Brown DW, Lee T, Vaughan MM, Alexander NJ, Busman M, Gutiérrez S (2018) Evolution of structural diversity of trichothecenes, a family of toxins produced by plant pathogenic and entomopathogenic fungi. PloS Pathogens. 14(4):e1006946. doi.org/10.1371/journal. ppat.1006946.

112. Holmes AJ, Tujula NA, Holley M, Contos A, James JM, Rogers P, Gillings MR (2001) Phylogenetic structure of unusual aquatic microbial formations in Nullarbor caves, Australia. Environmental Microbiology. 3:256–264. DOI: 10.1046/j.1462-2920.2001.00187.x.

113. Schabereiter-Gurtner C, Saiz-Jimenez C, Piñar G, Lubitz W, Rölleke S (2002) Phylogenetic 16S rRNA analysis reveals the presence of complex and partly unknown bacterial communities in Tito Bustillo cave, Spain, and on its Paleolithic paintings. Environmental Microbiology*.* 4:392–400. DOI: 10.1046/j.1462-2920.2002.00303.x.

114. Zhu H-Z, Zhang ZF, Zhou N, Jiang CY, Wang BJ, Cai L, Liu S-J (2019) Diversity, distribution and co-occurrence patterns of bacterial communities in a karst cave system. Frontiers in Microbiology. 10: 1726. doi.org/10.3389/fmicb.2019.01726.

115. Sjöberg S, Stairs CW, Allard B, Homa F, Martin T, Sjöberg V, Ettema TJG, Dupraz C. (2020) Microbiomes in a manganese oxide producing ecosystem in the Ytterby mine, Sweden: impact on metal mobility. FEMS Microbiology Ecology. 96: doi.org/10.1093/femsec/fiaa169.

116. Barriuso J, Márin S, Mellado RP (2010) Effects of the herbicide glyphosate-tolerant maize rhizobacteria communities: a comparison with pre-emergency applied herbicide consisting of a combination of acetochlor and terbuthylazine. Environmental Microbiology. 12:1021-1030. DOI: 10.1111/j.1462-2920.2009.02146.x.

117. Bian X, Xiao S, Zhao Y, Xu Y, Yang H, Zhang L (2020) Comparative analysis of rhizosphere soil physiochemical characteristics and microbial communities between rusty and healthy ginseng root.

Scientific Reports. 10:15756. doi.org/10.1038/s41598-020-71024-8.

118. Nusslein K, Tiedje JM (1999) Soil bacterial community shift correlated with change from forest to pasture vegetation in a tropical soil. Applied and Environmental Microbiology. 65:3622–3626. DOI:10.1128/AEM.65.8.3622-3626.1999.
119. Köberl M, Dita M, Martinuz A, Staver C, Berg G (2017) Member of Gammaproteobacteria as indicator species of healthy banana plants on Fusarium wilt-infested fields in Central America. Scientific Reports. 7:45318. doi.org/10.1038/srep45318.
120. Byers A-K, Condron L, O'Callaghan M, Waipara N, Black A (2020) Soil microbial community restructuring and functional changes in ancient kauri (*Agathis australis*) forest impacted by the invasive pathogen *Phytophthora agathidicida*. Soil Biology and Biochemistry. 150:108016. https://doi.org/10.1016/j.soilbio.2020.108016.
121. Przemieniecki SW, Damszel M, Ciesielski S, Kubiak K, Mastalerz J, Sierota Z, Gorczyca A (2021) Bacterial microbiome in *Armillaria ostoyae* rhizomorphs inhabiting the root zone during progressively dying Scots pine. Applied Soil Ecology. 164:103929. doi.org/10.1016/j.apsoil.2021.103929.
122. Saccá ML, Manici LM, Caputo F, Frisullo S (2019) Changes in rhizosphere bacterial communities associated with tree decline: grapevine esca syndrome case study. Canadian Journal of Microbiology. 65:930-943. doi.org/10.1139/cjm-2019-0384.
123. Liu J, He X, Sun J, Ma Y (2021) A degeneration gradient of poplar trees contributes to the taxonomic, functional, and resistome diversity of bacterial communities in rhizosphere soils. International Journal of Molecular Sciences. 22:3438. doi.org/10.3390/ijms22073438.
124. Tong A-Z, Liu W, Liu Q, Xia G-Q, Zhu J-Y (2021) Diversity and composition of the Panax ginseng rhizosphere microbiome in various cultivation modes and ages. BMC Microbiology. 21: 18. https://doi.org/10.1186/s12866-020-02081-2.
125. Balestrini R, Lumini E, Borriello R, Biancotto V (2014) Plant-soil biota interactions. In: E.A. Paul (4th ed.), *Soil Microbiology, Ecology, and Biochemistry*. Cambridge, MA: Academic Press. p. 311-338. eBook ISBN: 9780123914118. https://doi.org/10.1016/C2011-0-05497-2.
126. Horton BW, Glen M, Davidson NJ, Ratkowsky D, Close DC, Wardlaw TJ, Mohammed C (2013) Temperate eucalypt forest decline is linked to altered mycorrhizal communities mediated by soil chemistry. Forest Ecology and Management. 302:329-337. DOI: 10.1016/j.foreco.2013.04.006.
127. Kipfer T, Egli S, Ghazoul J, Moser B, Wohlgemuth T (2010) Susceptibility of ectomycorrhizal fungi to soil heating. Fungal Biology. 114: 467-472. doi: 10.1016/j.funbio.2010.03.008.
128. Rudawska M, Leski T, Stasinska M (2011) Species and functional diversity of ectomycorrhizal fungal communities on Scots pine (*Pinus sylvestris* L.) trees on three different sites. Annual of Forest Science. 68: 5-15. DOI:10.1007/s13595-101-0002-x.

Figures

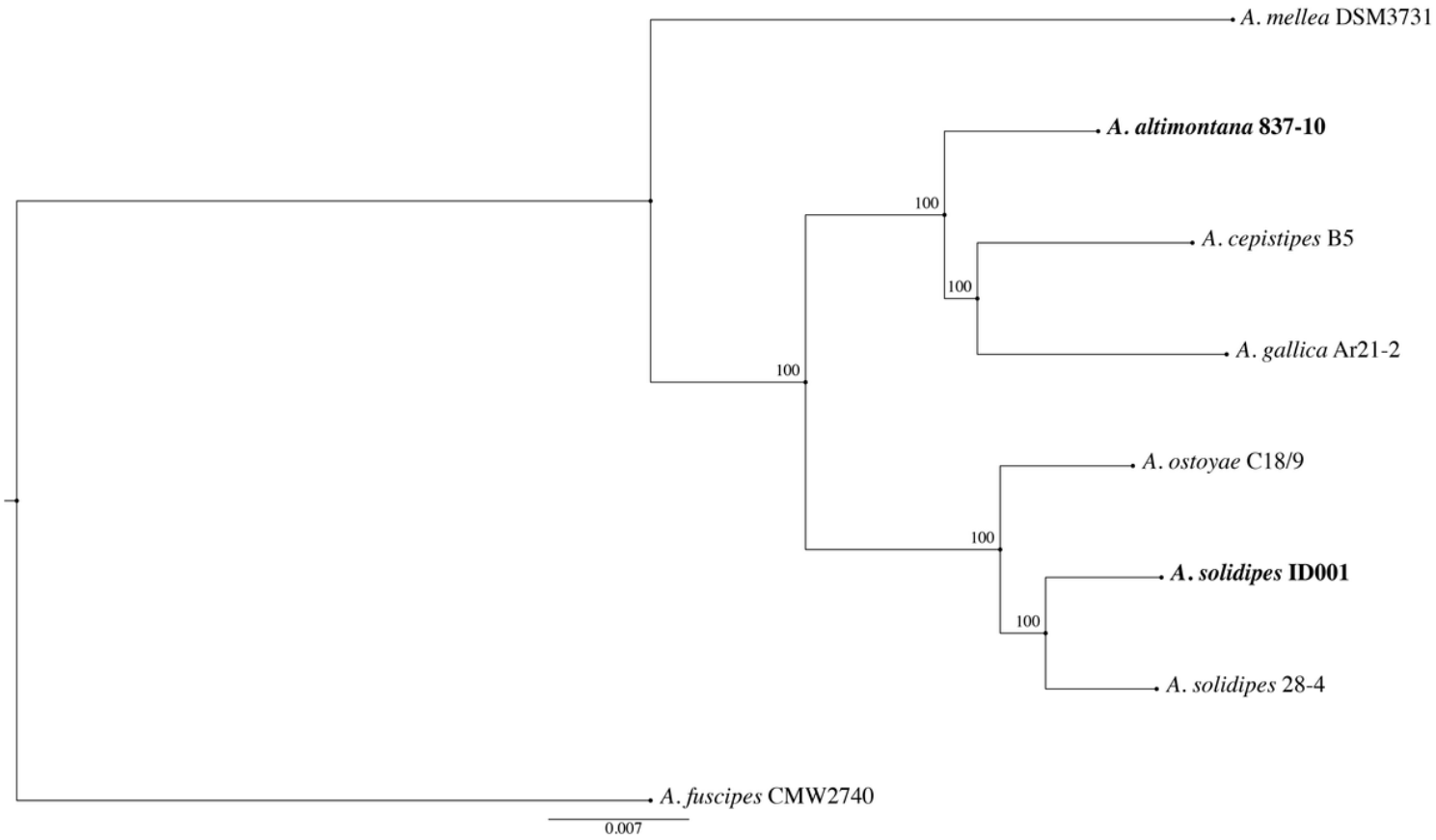

Figure 1

Whole genome phylogenetic tree of Armillaria species: Armillaria mellea DSM3731 [France], A. altimontana 837-10 [Idaho], A. cepistides B5 [Italy], A. gallica Ar21-2 [Vermont], A ostoyae C18/9 [Switzerland], A. solidipes ID001 [Idaho], and A. solidipes 28-4 [Vermont].

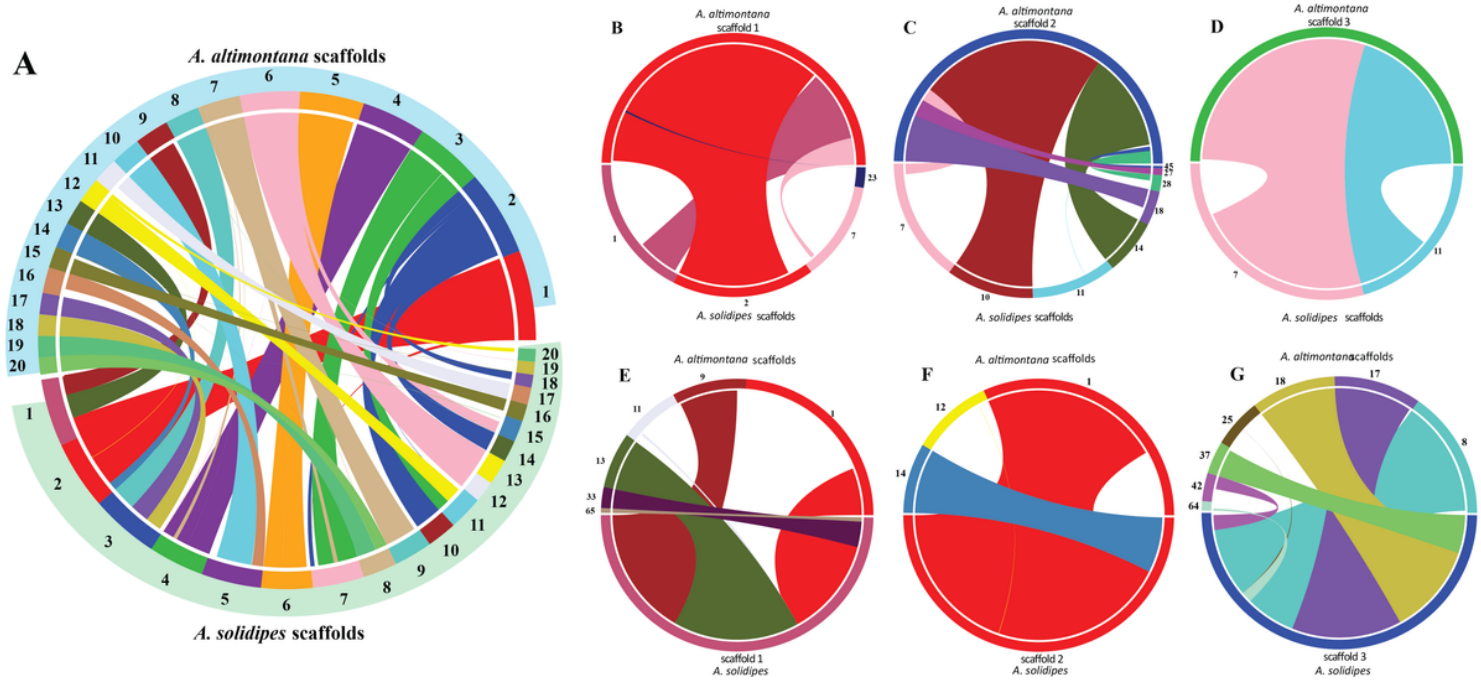

Figure 2

Blocks of synteny comparing the 20 largest scaffolds of each Armillaria species (A); B-D: block of synteny of the three largest A. altimontana scaffolds with A. solidipes scaffolds; E-G: blocks of synteny of the three largest A. solidipes scaffolds with A. altimontana scaffolds.

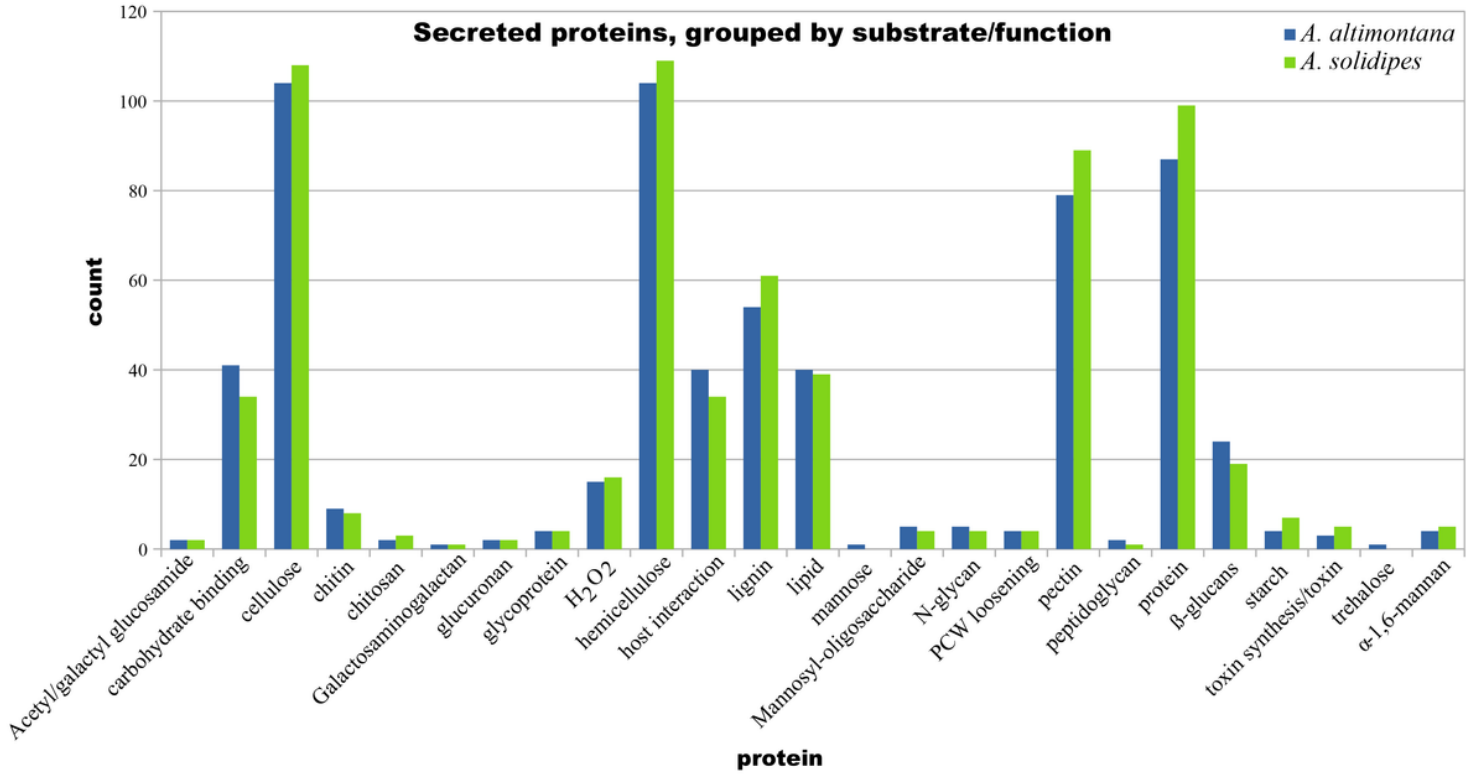

Figure 3

Comparison of the number of pathogenicity-related secreted proteins in Armillaria altimontana and A. solidipes, grouped by function. Small secreted proteins are not included. All CBM genes were considered with a “carbohydrate binding” function.

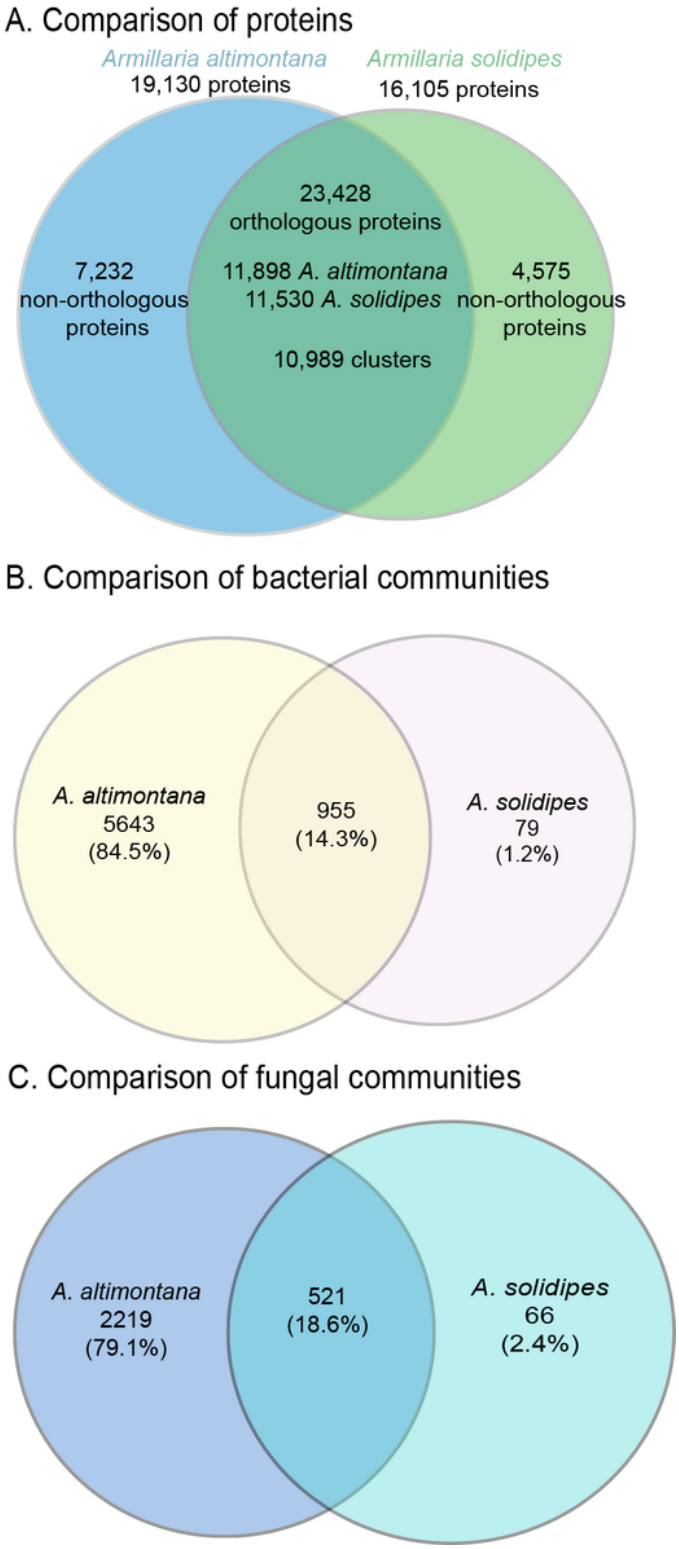

Figure 4

A. Orthologous and non-orthologous proteins of the two Armillaria species. Microbial communities (OTUs) between A. altimontana and A. solidipes. 4 B,C. Core microbiome encompasses overlap between both species, while unique OTUs occur within each circle for B . Unique OTUs occur within each of the three circles; 4B. bacterial communities. C. Fungal communities.

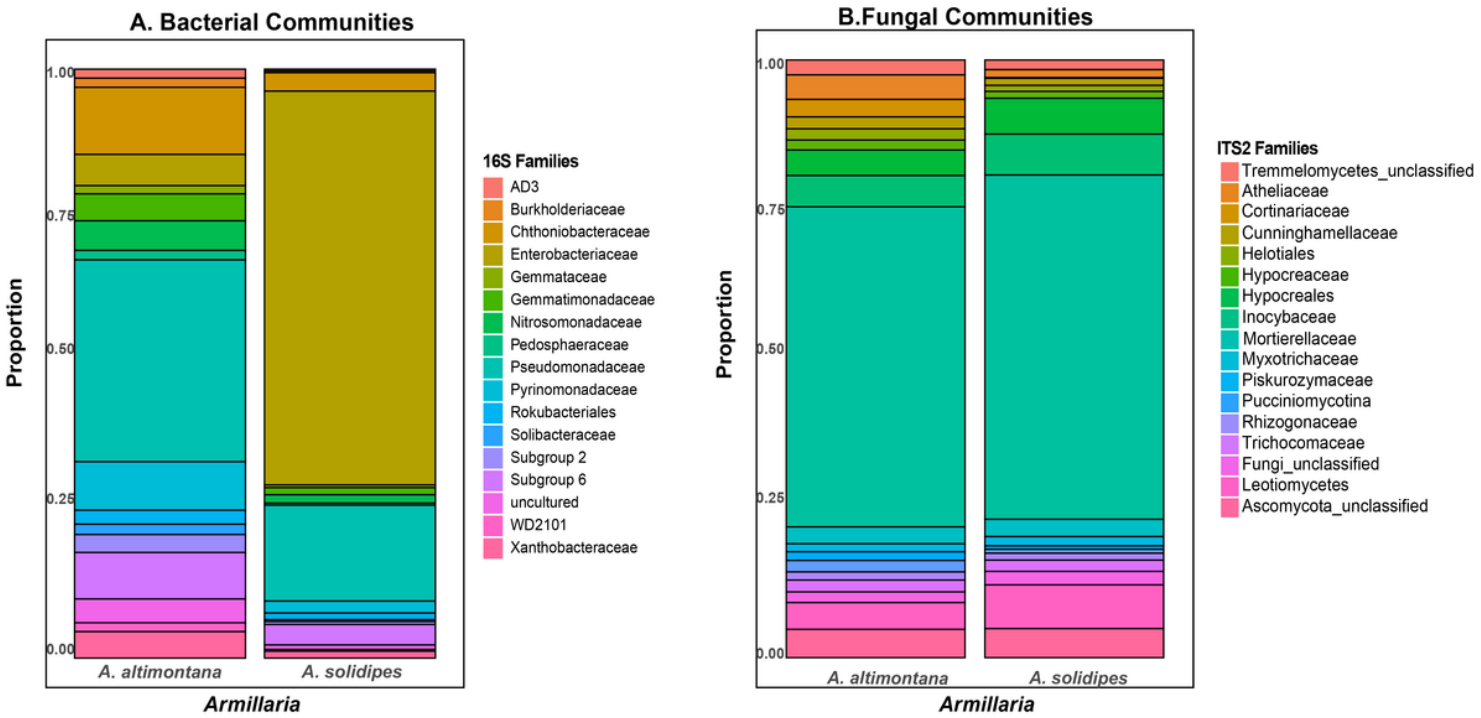

Figure 5

Stacked bar graphs of top 17 most abundant bacterial families (A) and fungal families (B) for Armillaria altimontana and A. solidipes.

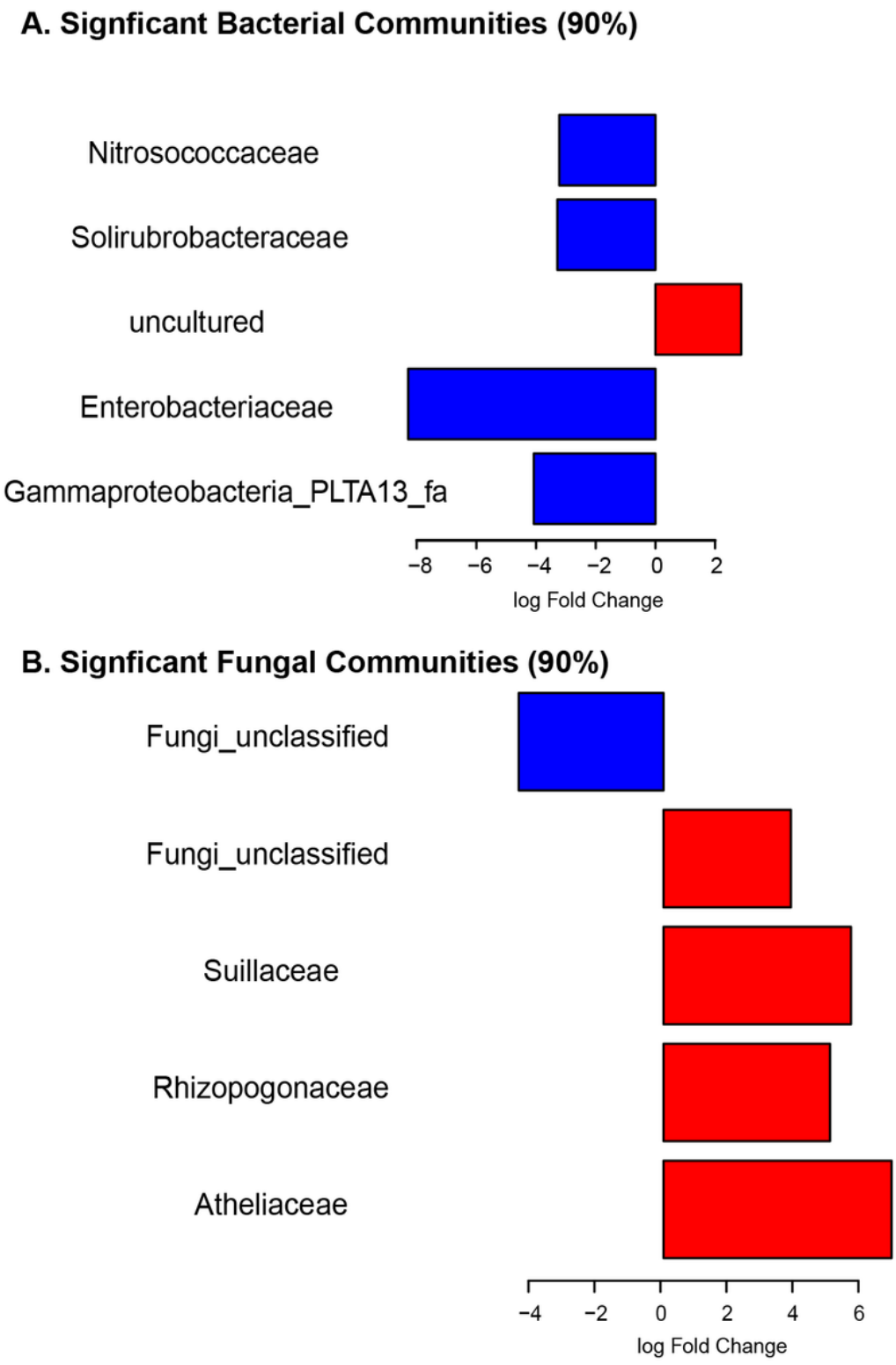

Figure 6

Log fold change for unique bacterial (A) and Fungal (B) OTUs in association between A. altimontana (red) and A. solidipes (blue). Significance is based on 90% confidence log fold change between both species of Armillaria.

Supplementary Files

This is a list of supplementary files associated with this preprint. Click to download.

- SupplementalTables.docx
- SupplementalFigure1.pdf
- SupplementalFigure2secretedproteinsbothhorizontalnoGH0.pdf
- SupplementalFigure3nonsecretedcazymesgrouped.pdf
- SupplementalFigure4abRarefractions.pdf
- SupplementalFigure5PCoA16SITS.pdf